

---

# 19 High-Permeability Fracturing

**Ronald E. Oligney**  
*Texas A&M University*

**Peter Valkó**  
*Texas A&M University*

**Michael J. Economides**  
*Texas A&M University*

**Sanjay Vitthal**  
*Halliburton Energy Services*

---

## 19-1 INTRODUCTION

Since it was first used to improve production from marginal wells in Kansas in 1946, and its rapid, widespread acceptance in the early 1950s, massive hydraulic fracturing (MHF) has become the dominant completion technique in the U.S. In 1993, 40% of new, completed oil wells and 70% of gas wells were fracture-treated (Figure 19-1). With improved modern fracturing capabilities and the advent of high-permeability fracturing (HPF), also referred to as a *fracpack* or other variants, the industry is increasingly recognizing the tremendous advantages of fracturing most wells. Even near water or gas contacts, prospects considered the bane of fracturing, HPF is being applied, because it offers controlled fracture extent and limits drawdown (Mullen *et al.*, 1996; Martins *et al.*, 1992).

The rapid ascent of high-permeability fracturing from a few isolated treatments before 1993 (Martins *et al.*, 1992; Grubert, 1990; Ayoub *et al.*, 1992) to some 300 treatments per year in the U.S. by 1996 (Tiner *et al.*, 1996) suggests that HPF is becoming a dominating optimization tool for integrated well completion and production and one of the major recent developments in petroleum production (Table 19-1).

As recently as 1993, hydraulic fracturing was considered simply a means of production enhancement, and was used almost exclusively for low-permeability reser-

voirs. The large fluid leakoff and unconsolidated sands associated with high-permeability formations would ostensibly prevent the initiation and extension of a single, planar fracture with sufficient width to accept a meaningful proppant volume. Moreover, such fracture morphology, even if successfully created and propped, would be incompatible with the defined needs of moderate- to high-permeability reservoirs, which require large conductivity (width).

The key feature in high-permeability fracturing is the tip-screenout (TSO) technique, which arrests lateral fracture growth and allows for subsequent fracture inflation and packing. The result is short but exceptionally wide fractures. While in traditional, unrestricted fracture growth, an average fracture width of 0.25 in. would be considered normal, in TSO treatments, widths of 1 in. or even larger are commonly discussed.

Fundamental modeling and field evidence have suggested that HPF treatments are primarily effective because they bypass near-well damage (DeBonis *et al.*, 1994; Grubert, 1990; Hannah *et al.*, 1993; Hunt *et al.*, 1994; Martins *et al.*, 1992; Montagna *et al.*, 1995; Monus *et al.*, 1992; Mullen *et al.*, 1994; Patel *et al.*, 1994; Reimers and Clausen, 1991; Smith *et al.*, 1987; Stewart *et al.*, 1995a and 1995b; Wong *et al.*, 1993). This benefit is both the controlling and the necessary mechanism for appreciable production enhancements from HPF jobs.

Fundamentally, high-permeability fracturing would always result in a negative skin effect, although it would be of much smaller absolute value than the skins

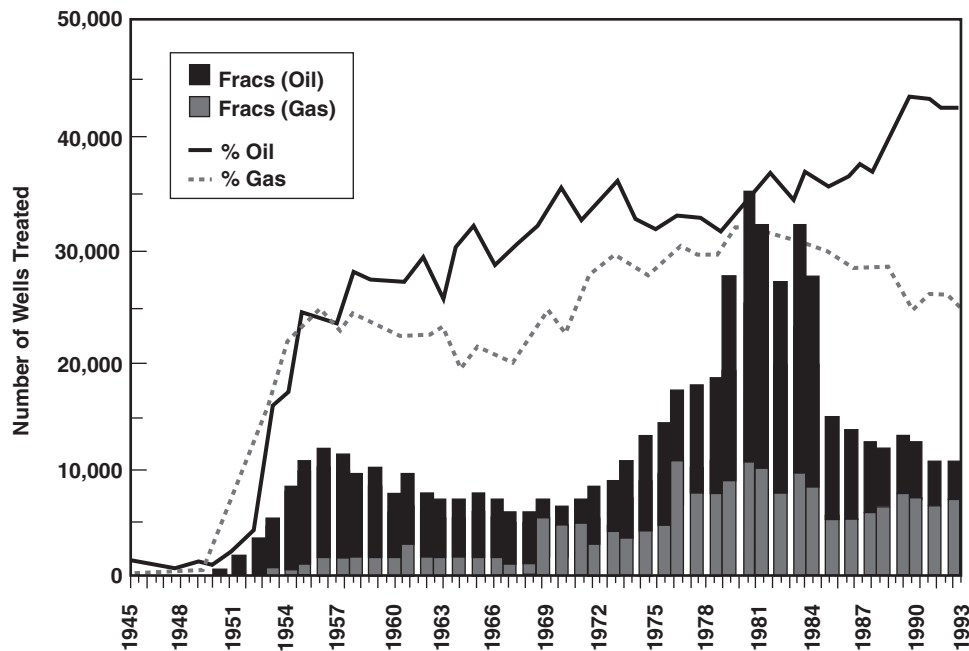


Figure 19-1 The importance of hydraulic fracturing

obtained in low-permeability reservoirs. However, post-treatment positive skins have been measured in many wells, and these must be attributed to the connectivity (choke) between the well and the fracture. This connectivity is related, for instance, to the number and condition of the perforations, and the fracture tortuosity from its initiation direction to its ultimate propagation direction. These issues are addressed in Section 19-6.3 because, although they affect all fractures, they have a particularly serious effect on the low conductivity expected in high-permeability treatments. Thus, although from an “accounting” point of view, a pretreatment skin effect of 10 compared to a post-treatment skin of 5 would imply a skin reduction equal to 5, in reality, the pretreatment skin of 10 is totally eliminated and supplanted by a new skin equal to 5. This issue is important because it suggests the direction of indicated improvements in these types of stimulation treatments.

Table 19-1 Fracturing role expanded

Permeability	Gas	Oil
Low	$k < 0.5 \text{ md}$	$k < 5 \text{ md}$
Moderate	$0.5 < k < 5 \text{ md}$	$5 < k < 50 \text{ md}$
High	$k > 5 \text{ md}$	$k > 50 \text{ md}$

While production enhancement is of primary importance, there are actually a number of reasons to consider fracturing a high-permeability formation:

- Bypassing formation damage
- Controlling sand deconsolidation
- Reducing fines migration and asphaltene production
- Reducing bottom water coning
- Improving communication between reservoir and wellbore
- Stimulating wells

In contrast to virtually all conventional hydraulic fracturing, positive post-treatment skin effects are possible after HPF treatments. This effect is commonly attributed to fracture-face damage that results from excessive fluid leakoff, but non-Darcy flow in the formation and especially in the fracture may also be a reasonable hypothesis.

It is interesting that HPF (fracpack) treatments did not necessarily originate as an extension of hydraulic fracturing—although they borrowed heavily from established techniques—but rather as a means of sand-production control. In controlling the amount of surface sand production, two distinctly different activities can be performed downhole: *sand exclusion* and *sand*

*deconsolidation control.* Sand exclusion refers to all filtering devices such as screens and gravel packs. Gravel-packing, the historically preferred well completion method to remedy sand production, is one such technique. These techniques do not prevent sand migration in the reservoir, so fines migrate and lodge in the gravel pack and screen, causing large damage skin effects. Well performance progressively deteriorates and is often not reversible with matrix stimulation treatments. Attempts to stem the loss in well performance by increasing the pressure drawdown often aggravates the problem further and may potentially lead to wellbore collapse.

A more robust approach is the control of sand deconsolidation, the prevention of fines migration at the source. It is widely perceived that the use of HPF accomplishes this by mating with the formation in its (relative) undisturbed state and reducing fluid velocities or “flux” at the formation face.

Actually, three factors contribute to sand deconsolidation: (1) *pressure drawdown* and the resulting flux of the fluid, (2) the *strength of the rock* and integrity of the natural cementation, and (3) the *state of stress*. Of these three, the only factor that can be readily altered is the distribution of flow and pressure drawdown. With the introduction of formation fluids to the well along a more elongated path, such as a hydraulic fracture or horizontal well, it is entirely possible to reduce the fluid flux and, in turn, control sand production.

Of course, little can be done to affect the state of stress. The magnitude of earth stresses depends primarily on reservoir depth and to some extent, pressure, and the situation becomes more complicated at depths of 3000 ft or less. Pressure maintenance with gas or water flooding may be counterproductive unless maintenance of reservoir pressure allows economic production at a smaller drawdown. While various innovations have been suggested to remedy the incompetent formations or improve on natural cementation—for example, by introducing complex well configurations (Section 19-8.2) or various exotic chemical treatments—relatively little can be done to control this factor, either. Rock mechanics issues were discussed more broadly in Chapter 6.

In light of the discussion above, it should not be surprising that HPF is rapidly replacing gravel packs in many petroleum provinces that are susceptible to sand production. As with any stimulation technique that results in a productivity index improvement (defined as the production rate divided by the pressure drawdown), the operator is responsible for allocating this new pro-

ductivity index either to a *larger rate* or a *lower drawdown*, or any combination of the two.

The present trend in HPF indicates a marked departure from the heritage of gravel-packing, incorporating more and more from hydraulic-fracture technology. This trend can be seen, for instance, in the fluids and proppants applied. While the original fracpack treatments involved sand sizes and “clean” fluids common in gravel-packing, now the typical proppant size for hydraulic fracturing (20/40-mesh) seems to be dominant. The increasing application of crosslinked fracturing fluids also supports the trend.

For this reason, the term *high-permeability fracturing* (HPF) seems more appropriate than *fracpack*, and this term will be used throughout the chapter.

In the following section, HPF is compared in a semi-quantitative way to competing technologies. This comparison is followed by a discussion of the key issues in high-permeability fracturing including design, execution, and evaluation.

## 19-2 HPF VS. COMPETING TECHNOLOGIES

### 19-2.1 Gravel Pack

The term *gravel pack* refers to the placement of gravel (actually, carefully selected and sized sand) between the formation and the well as a means of filtering out (retaining) reservoir particles that migrate through the porous medium. A “screen” is used to hold the gravel pack itself in place. This manner of excluding reservoir fines from flowing into the well causes an accumulation of fines in the near-well zone and an attendant reduction in gravel-pack permeability (i.e. damage).

The progressive deterioration of gravel-pack permeability (increased skin effect) leads, in turn, to a decline in well production. Increasing the pressure drawdown to counteract production losses can result in accelerated pore-level deconsolidation and additional sand production.

Any productivity index relationship, e.g. the steady-state expression for oil, can be used to demonstrate this point:

$$J = \frac{q}{p_e - p_{wf}} = \frac{kh}{141.2B\mu \left( \ln \frac{r_e}{r_w} + s \right)} \quad (19-1)$$

If we assume that  $k = 50$  md,  $h = 100$  ft,  $B = 1.1$  res bbl/STB,  $\mu = 0.75$  cp and  $\ln r_e/r_w = 8.5$ , the productivity indexes for an ideal (undamaged), a relatively damaged ( $s = 10$ ), and a typical gravel-packed well ( $s = 30$ ) would

be 5, 2.3 and 1.1 STB/d/psi, respectively. For a drawdown of 1,000 psi, these productivity indexes would result in production rates of 5000, 2300 and 1100 STB/d, respectively. Clearly, the difference in production rates between the ideal and gravel-packed wells can be considerable and very undesirable.

High-permeability fracturing under the same scenario would combine the advantages of propped fracturing to bypass the near-wellbore damage and gravel-packing to provide effective sand control. Figure 19-2 is the classic presentation of fracture-equivalent skin effect (Cinco-Ley *et al.*, 1978) in terms of dimensionless fracture conductivity,  $C_{fD}(=k_f w/kx_f)$ , and the fracture half-length,  $x_f$ .

As shown in Figure 19-2, even with a lackluster hydraulic fracture ( $C_{fD} = 0.5$ ) and short fracture length ( $x_f = 50$  ft), the skin effect,  $s_f$  (using again  $r_w = 0.328$  ft), would be equal to  $-3$ .

A negative skin effect equal to  $-3$  applied to Equation 19-1 yields a productivity index of 7.7 STB/d/psi, more than a 50% increase over the ideal PI, and seven times the magnitude of a damaged gravel-packed well. Even with a damaged fracture (leakoff-induced damage as described by Mathur *et al.*, 1995) and a skin equal to  $-1$ , the productivity index would be 5.6 STB/d/psi, a five-fold increase over a damaged gravel-packed well.

This calculation brings forward a simple, yet frequently overlooked issue. Small negative skin values have a much greater impact on well performance than comparable magnitudes (absolute value) of positive skin. Furthermore, in the example calculation, a five-fold increase in the productivity index suggests that the production rate would increase by the same amount if the drawdown is held constant. Under an equally possible scenario, the production rate could be held constant and the drawdown reduced to  $\frac{1}{5}$  its original value. Any other combination between these two limits can be envisioned. The utility of high-permeability fracturing is, thus, compelling.

### 19-2.2 High-Rate Water Packs

As shown in Table 19-2, distilled from recent empirical data collected and reported by Tiner *et al.* (1996), high-

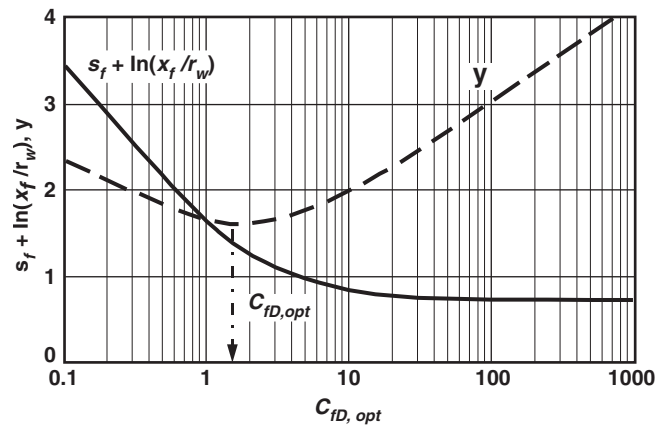


**Figure 19-2** Pseudoskin factor of a vertical well intersected by a finite-conductivity vertical fracture (after Cinco-Ley *et al.*, 1978)

rate water packs seem to have an advantage over gravel packs, but they do not provide the productivity improvement of HPF. This improvement over gravel packs is reasonable because of the additional proppant placed in the perforation tunnels.

While not shown in the table, the performance of these completions over time is also of interest. It is commonly reported that production from high-rate water packs (as in the case of gravel packs) deteriorates with time. By contrast, Stewart *et al.* (1995), Mathur *et al.* (1995), and Ning *et al.* (1995) all report that production may progressively improve (skin values may decrease) during the first several months after an HPF treatment.

### 19-2.3 Performance of Fractured Horizontal Wells in High-Permeability Formations

Two of the most important recent developments in petroleum production are horizontal wells and high-permeability fracturing. Considerable potential is possible when the two technologies are combined. Horizontal wells can be drilled either transversely or longitudinal to the fracture azimuth. The transverse configuration is appropriate for low-permeability formations and has been widely used and documented in the literature. The longitudinally fractured horizontal well warrants further attention, specifically in the case of high-permeability

**Table 19-2** Skin values reported by Tiner *et al.* (1996)

Gravel-pack	High-Rate Water Pack	HPF
+5 to +10, excellent	+2 to +5, reported	0 to +2, normally
+40 and higher are reported		

**Table 19-3** Discounted revenue in \$ millions US

Configuration	$k = 1$ md	$k = 10$ md	$k = 100$ md
Vertical well	0.73	6.4	57.7
Horizontal well	3.48	14.2	78.8
Fractured vertical well, $C_{fD} = 1.2$	2.59	13.4	89.6
Fractured horizontal well, $C_{fD} = 1.2$	3.88	16.3	95.8
Infinite-conductivity fracture (upper bound for both horizontal and vertical well cases)	3.91	16.3	103.3

formations. HPF often results in low dimensionless-conductivity hydraulic fractures, yet such fractures installed longitudinally in horizontal wells in high-permeability formations can have the net effect of installing a (relative) high-conductivity streak in an otherwise limited-conductivity flow conduit. Using a generic set of input data, Valkó and Economides (1996) showed discounted revenues for 15 cases that demonstrate this point.

Table 19-3 shows that for a given permeability, the potential for the longitudinally fractured horizontal well is always higher than that of a vertical well, and that the horizontal well may approach the theoretical potential of an infinite-conductivity fracture when realistic fracture widths are considered.

Furthermore, Valkó and Economides showed that the horizontal well fractured with 10-fold less proppant ( $C_{fD} = 0.12$ ) still outperforms the fractured vertical well for  $k = 1$  and 10 md, and that the horizontal well is competitive at 100 md. In fact, for the range of 1 to 10 md, even a 100-fold reduction in fracture width ( $C_{fD} = 0.012$ ) is more than enough. Thus, with the longitudinal configuration, orders-of-magnitude less fracture width (than that suggested for a fractured vertical well) might be sufficient to achieve a certain production goal.

(and assuming the pump rate is larger than the rate of leakoff to the formation), continued pumping will inflate the fracture (increase fracture width). This TSO and fracture inflation should be accompanied by an increase in net fracture pressure. Thus, the treatment can be conceptualized in two distinct stages: fracture creation (equivalent to conventional designs) and fracture inflation/packing (after tip-screenout).

Figure 19-4 (after Roodhart *et al.*, 1993) compares the two-stage HPF process with the conventional single-stage fracturing process. Creation of the fracture and the arrest of its growth (tip-screenout) is accomplished by injecting a relatively small pad and a 1 to 4-lb/gal sand slurry. Once fracture growth has been arrested, further injection builds fracture width and allows injection of high-concentration (10 to 16-lb/gal) slurry. Final areal proppant concentrations of 20 lb/ft<sup>2</sup> are not uncommon. The figure also illustrates the common practice of retarding injection rate near the end of the treatment (coincidental with opening the annulus to flow) to dehydrate/pack the near wellbore and screen. Rate reductions may also be used to force tip-screenout in cases where no TSO event is observed on the downhole pressure record.

## 19-3 KEY ISSUES IN HPF

### 19-3.1 Tip-Screenouts

The critical elements of high-permeability fracturing treatment design, execution, and interpretation are substantially different than for conventional fracturing treatments. In particular, HPF relies on a carefully timed *tip-screenout* (TSO) to limit fracture growth and allow for fracture inflation and packing (Figure 19-3). The TSO occurs when sufficient proppant has concentrated at the leading edge of the fracture to prevent further fracture extension. Once fracture growth has been arrested

**Figure 19-3** Width inflation with the tip-screenout technique

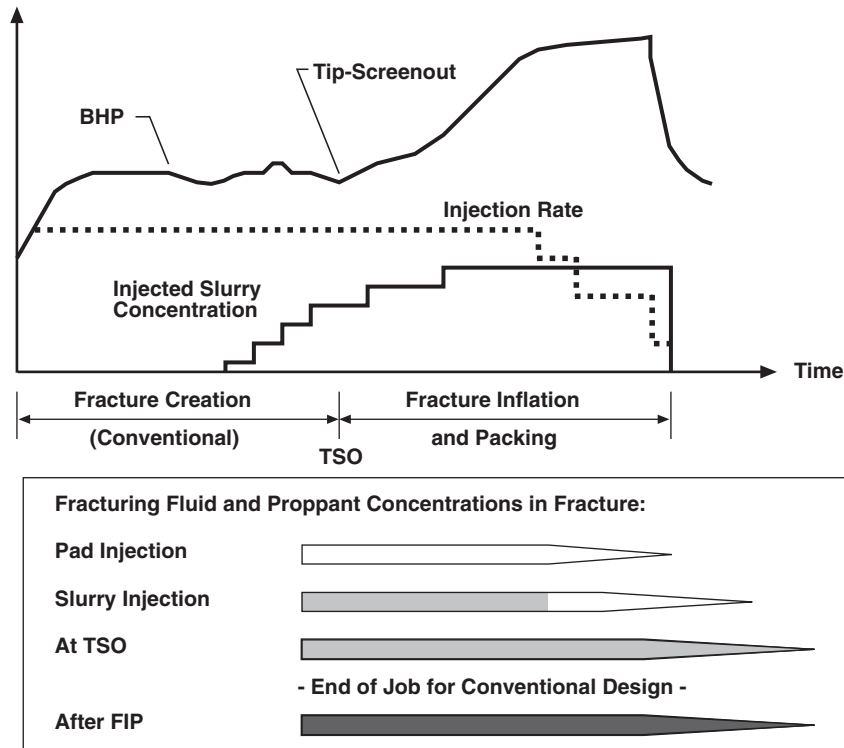


Figure 19-4 Comparison of conventional and HPF design concepts (after Roodhart *et al.*, 1993)

Industry experience suggests that the tip-screenout can be difficult to model, affect, or even detect. The many reasons for this difficulty include a tendency toward overly conservative design models (resulting in no TSO), partial or multiple tip-screenout events, and inadequate pressure monitoring practices.

It is now well accepted that accurate bottomhole measurements are imperative for meaningful treatment evaluation. Calculated bottomhole pressures are unreliable because of the dramatic friction pressure effects associated with pumping high sand concentrations through reduced-ID tubulars and service-tool crossovers. Surface data may indicate that a TSO event has occurred when the bottomhole data shows no evidence, or the opposite may be true. Even in the case of downhole pressure data, there has been some discussion regarding where measurements should be taken. Friction and turbulence concerns have caused at least one operator to conclude that bottomhole pressure data should be collected from below the crossover tool (washpipe gauges) in addition to the data collected from the service tool bundle (Mullen *et al.*, 1994).

The detection of tip-screenout is discussed further in Section 19-7 along with the introduction of a simple screening tool to evaluate bottomhole data.

### 19-3.2 Net Pressure and Fluid Leakoff Considerations

The entire HPF process is dominated by net pressure and fluid leakoff considerations, first because high-permeability formations are typically soft and exhibit low elastic modulus values, and second, because the fluid volumes are relatively small and leakoff rates are high (high permeability, compressible reservoir fluids, and non-wall-building fracturing fluids). As described previously, the tip-screenout design itself also affects net pressure. While traditional practices applicable to design, execution, and evaluation in MHF continue to be used in HPF, these are frequently not sufficient.

#### 19-3.2.1 Net Pressure, Closure Pressure, and Width in Soft Formations

Net pressure is the difference between the pressure at any point in the fracture and the fracture closure pressure. This definition involves the existence of a unique closure pressure. Whether the closure pressure is a constant property of the formation, or it depends heavily on the pore pressure (or rather on the disturbance of the pore

pressure relative to the long-term steady value) is an open question.

In high-permeability, soft formations, it is difficult (if not impossible) to suggest a simple recipe to determine the closure pressure as classically derived from shut-in pressure decline curves (Section 19-4.3.2). Furthermore, because of the low elastic modulus values, even small, induced uncertainties in the net pressure are amplified into large uncertainties in the calculated fracture width.

### 19-3.2.2 Fracture Propagation

Fracture propagation, the availability of sophisticated 3D models notwithstanding, is not yet a well-described phenomenon. Recent studies (Chudnovsky *et al.*, 1996) emphasize the stochastic character of this propagation in competent hard-rock formations. No serious attempt has been made to describe the physics of fracture propagation in soft rock, but it is reasonably expected to involve incremental energy dissipation and more severe tip effects (with the effect of increasing net pressures). Again, because of the low modulus values, an inability to predict net-pressure behavior may lead to significant differences between predicted and actual treatment performance. Ultimately, the classic models may not reflect even the main features of the propagation process.

Currently, fracture propagation and net-pressure features are “predicted” through the use of a computer fracture-simulator. This trend of substituting clear models and physical assumptions with “knobs” such as (1) arbitrary stress barriers, (2) friction changes (attributed to erosion, if decreasing, and sand resistance, if increasing) and (3) poorly understood properties of the formation expressed as dimensionless “factors,” does not help clarify the issue.

### 19-3.2.3 Leakoff in the High-Permeability Environment

Considerable effort has been expended on laboratory investigation of the fluid leakoff process for high-permeability cores. A comprehensive report can be found in both Vitthal and McGowen (1996) and McGowen and Vitthal (1996). The results raise some questions about how effectively fluid leakoff can be limited by filter-cake formation.

In all cases, but especially in high-permeability formations, the quality of the fracturing fluid is only one of the factors that influence leakoff, and it is often not the determining one. Transient fluid flow in the formation

might have an equal or even larger impact. Transient flow cannot be understood by simply fitting an empirical equation to laboratory data; the use of models based on solutions to the fluid flow in porous media is an unavoidable step.

## 19-3.3 Fundamentals of Leakoff in HPF

In the following, three models are considered that describe leakoff in the high-permeability environment. Use of the traditional Carter leakoff model requires some modification for use in HPF as shown. (Note: While this model continues to be used almost exclusively across the industry, it is not entirely sufficient for the HPF application.) An alternate, filter cake-based leakoff model has been developed based on the work by Mayerhofer *et al.* (1993). The most appropriate but not yet widespread leakoff model for high-permeability formations may be that of Fan and Economides (1995), which considers the series resistance caused by (1) the filter cake, (2) the polymer-invaded zone, and (3) the reservoir. While the Carter model is the most common in current use, the models of Mayerhofer *et al.* and Fan and Economides represent important building blocks and provide a conceptual framework for understanding the critical issue of leakoff in HPF.

### 19-3.3.1 Fluid Leakoff and Spurt Loss as Material Properties: The Carter Leakoff Model with Nolte's Power Law Assumption

To make use of material balance, the term  $V_L$ , the lost volume, must be described. For rigorous theoretical development,  $V_L$  is the volume of liquid entering the formation through the two created fracture surfaces of one wing. There are two main philosophies concerning leakoff. The first considers the phenomenon as a *material property* of the fluid/rock system. The basic relation (called the integrated Carter equation, also provided in Chapter 17) is given in consistent units as

$$\frac{V_L}{A_L} = 2C_L\sqrt{t} + S_p \quad (17-18)$$

where  $A_L$  is the area and  $V_L$  is the total volume lost during the period from time zero to time  $t$ . The integration constant,  $S_p$ , is called the spurt-loss coefficient, which is measured in meters. It can be considered as the *width* of the fluid body passing through the surface instantaneously at the very beginning of the leakoff process, while  $2C_L\sqrt{t}$  is the width of the fluid body following

the first slug. The two coefficients,  $C_L$ , and  $S_p$  can be determined from laboratory tests.

As discussed in more detail in Chapter 17, Equation 17-18 can be visualized assuming that the given surface element “remembers” when it has been opened to fluid loss and has its own “zero” time, which might be different from location to location on a fracture surface. Points of the fracture face near to the well are opened at the beginning of pumping while the points at the fracture tip are “younger.” Application of Equation 17-18 or of its differential form necessitates the tracking of the opening time of the different fracture-face elements, as discussed in Chapter 17.

The second philosophy considers leakoff as a consequence of flow mechanisms into the porous medium and uses a corresponding mathematical description.

### 19-3.3.2 Filter Cake Based Leakoff Model According to Mayerhofer et al.

The method of Mayerhofer *et al.* (1993) describes the leakoff rate using two parameters that are physically more realistic than the leakoff coefficient: (1) filter-cake resistance at a reference time and (2) reservoir permeability. It is assumed that these parameters ( $R_0$ , the reference resistance at a reference time  $t_0$ , and  $k_r$ , the reservoir permeability) have been identified from a minifrac diagnostic test. In addition, reservoir pressure, reservoir fluid viscosity, porosity, and total compressibility are assumed to be known.

Total pressure gradient from inside a created fracture out into the reservoir,  $\Delta p$ , at any time during the injection, can be written as

$$\Delta p(t) = \Delta p_{\text{face}}(t) + \Delta p_{\text{piz}}(t) + \Delta p_{\text{res}}(t) \quad (17-26)$$

where  $\Delta p_{\text{face}}$  is the pressure drop across the fracture face dominated by the filter cake,  $\Delta p_{\text{piz}}$  is the pressure drop across a polymer-invaded zone, and  $\Delta p_{\text{res}}$  is the pressure drop in the reservoir. This concept is shown in Figure 19-5.

In a series of experimental works using typical hydraulic fracturing fluids (e.g. borate and zirconate-crosslinked fluids) and cores of permeability less than 5 md, no appreciable polymer-invaded zone was detected. This simplifying assumption is not valid for linear gels such as HEC (which do not form a filter cake), and the assumption may break down for crosslinked fluids at higher permeabilities, (50 + md). Thus, at least for crosslinked fluids, the second term in the right side of Equation 17-26 can reasonably be ignored, yielding

$$\Delta p(t) = \Delta p_{\text{face}}(t) + \Delta p_{\text{res}}(t) \quad (19-2)$$

The filter-cake pressure term is proportional to  $R_0$ , the characteristic resistance of the filter cake. The transient pressure drop in the reservoir can be re-expressed as a series expansion of  $p_D$ , the dimensionless pressure function describing the behavior of the reservoir (unit response);  $t_D$  is the dimensionless time calculated with the maximum fracture length reached at time  $t_n$ , and  $r_p$  is the ratio of permeable height to the total height ( $h_p/h_f$ ). With rigorous introduction of these variables and considerable rearrangement (not shown), an expression for leakoff can be written that is useful for both hydraulic fracture propagation and fracture-closure modeling:

$$q_n = \frac{\Delta p(t_n) - \frac{\mu_r}{\pi k_r r_p h_f} \left[ -q_{n-1} p_D(t_{Dn} - t_{Dn-1}) + \sum_{j=1}^{n-1} (q_j - q_{j-1}) p_D(t_{Dn} - t_{Dj-1}) \right]}{\frac{R_0}{2r_p A_n} \sqrt{\frac{t_n}{t_e}} + \frac{\mu_r p_D(t_{Dn} - t_{Dn-1})}{\pi k_r r_p h_f}} \quad (19-3)$$

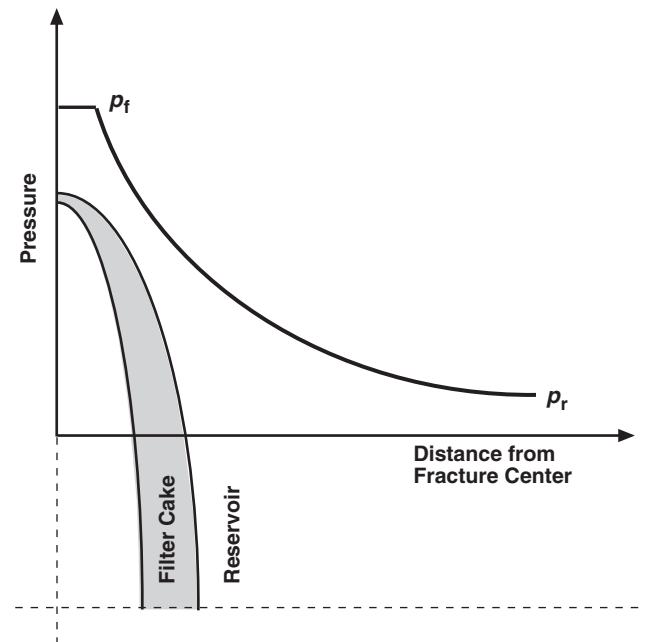


Figure 19-5 Filter cake plus reservoir pressure drop in the Mayerhofer *et al.* (1993) model

This expression allows for determination of the leakoff rate at time instant  $t_n$ , if the total pressure difference between the fracture and the reservoir is known, as well as the *history* of the leakoff process. The dimensionless pressure solution,  $p_D(t_{Dn} - t_{Dj-1})$ , has to be determined with respect to a dimensionless time that considers the *actual* fracture length at  $t_n$ .

The model can be used to analyze the pressure fall-off subsequent to a fracture injection (minifrac) test, as described by Mayerhofer *et al.* (1995). The method needs more input data than the similar analysis based on the Carter leakoff approach, but it offers the distinct advantage of differentiating between the two major factors of the leakoff process, filter-cake resistance and reservoir permeability.

### 19-3.3.3 Polymer-Invaded Zone-Based Leakoff Model of Fan and Economides

The leakoff model of Fan and Economides (1995) concentrates on the additional resistance created by the polymer-invaded zone. The total driving force behind fluid leakoff is the pressure difference between the fracture face and the reservoir,  $p_{\text{frac}} - p_i$ , which is equivalent to the sum of the following three separate pressure drops taken across the filter cake, in the polymer-invaded zone, and in the reservoir:

$$p_{\text{frac}} - p_i = \Delta p_{\text{cake}} + \Delta p_{\text{inv}} + \Delta p_{\text{res}} \quad (19-4)$$

The fracture treating pressure is equivalent to the net pressure plus fracture closure pressure (minimum horizontal stress). When a non-filter-cake fluid is used, the pressure drop across the filter cake is negligible, which is the case for many HPF treatments. The physical model of this situation, (i.e., fluid leakoff controlled by polymer invasion and transient reservoir flow), is depicted in Figure 19-6. The polymer invasion is labeled in the figure as Region 1, while the region of reservoir fluid compression (transient flow) is denoted as 2.

By employing conservation of mass, a fluid-flow equation, and an appropriate equation of state, a mathematical description of this fluid leakoff scenario can be written. As a starting point, Equation 19-5 describes power-law fluid behavior in the porous medium:

$$\frac{\partial^2 p}{\partial x^2} = \frac{n\phi\mu_{\text{eff}}c_t}{k} \left(\frac{1}{u}\right)^{1-n} \frac{\partial p}{\partial t} \quad (19-5)$$

where  $c_t$  is the system compressibility,  $k$  is the formation permeability,  $u$  is the superficial flow rate,  $n$  is the power law fluid-flow behavior index,  $\phi$  is the formation porosity, and  $\mu_{\text{eff}} = \frac{K'}{12} \left(9 + \frac{3}{n}\right)^n (150k\phi)^{\frac{1-n}{2}}$  is the fluid effective viscosity where  $K'$  is the power-law fluid consistency index.

Combining the description of the polymer-invaded zone and the reservoir, the total pressure drop is given by Fan and Economides (1995) as

$$p_{\text{frac}} - p_r = \frac{\sqrt{\pi}}{2} \frac{\phi\eta}{k} \left\{ \mu_{\text{app}} \sqrt{\alpha_1} e^{\left(\frac{\eta}{\sqrt{4\alpha_1}}\right)^2} \operatorname{erf}\left(\frac{\eta}{\sqrt{4\alpha_1}}\right) + \mu_r \sqrt{\alpha_2} e^{\left(\frac{\eta}{\sqrt{4\alpha_2}}\right)^2} \operatorname{erfc}\left(\frac{\eta}{\sqrt{4\alpha_2}}\right) \right\} \quad (19-6)$$

where

$$a_1 = \frac{k}{n\phi\mu_{\text{eff}} \left(\frac{1}{u}\right)^{1-n} c_t} \quad \text{and} \quad a_2 = \frac{k}{\phi\mu c_t}$$

At given conditions, Equation 19-6 can be solved iteratively for the variable  $\eta$ . Once the value of  $\eta$  is found for a specified total pressure drop, the leakoff rate is calculated from

$$q_L = A \left(\frac{\eta}{2\phi}\right) \frac{1}{\sqrt{t}} \quad (19-7)$$

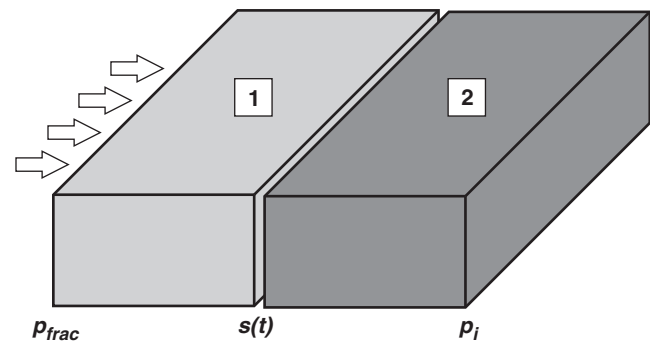


**Figure 19-6** Fluid leakoff model with polymer invasion and transient reservoir flow

In other words, the factor  $\eta/(2\phi)$  can be considered a pressure-dependent apparent leakoff coefficient.

#### 19-4 TREATMENT DESIGN AND EXECUTION

In contrast to the preceding section, which was quite theoretical (appropriately so) and dealt fundamentally with key issues involved in high-permeability fracturing, especially leakoff, this section will provide practical detail as to the current best practice being applied in HPF design and execution.

Most HPF treatments are done with mechanical sand control equipment in place. While this is not always the case, and while there are many potential variations, a generalized job sequence follows:

1. Perforate the formation.
2. Run the gravel-pack screen assembly.
3. Spot/soak acid to clean up perforations.
4. Perform and interpret pretreatment diagnostic tests.
5. Design the TSO pumping schedule based on design variables from diagnostic tests.
6. Pump the TSO treatment until screenout or until the volume needed to form an annulus pack remains in workstring.
7. Slow the pump rate to 1 to 2 bbl/min and open the annulus valve to circulate in and dehydrate an annular pack.
8. Shut down the pumps when tubing pressure reaches its safe upper limit.
9. Prepare the well for production.

##### 19-4.1 Perforations

It is widely agreed that establishing a conductive connection between the fracture and wellbore is critical to the success of HPF, but no consensus or study has emerged that gives definitive direction. In the context of high permeability and maximizing conductivity and fluid flow rate, a common response is to shoot the entire target interval with high shot-density and large holes (12 shots/ft with “big hole” charges). Concerns with clean formation breakdown (single-fracture initiation), near-well tortuosity, and perforations that are not packed with sand (especially in screenless HPFs) cause some operators to use just the opposite treatment: perforating the middle of the target zone only (possibly modifying the treatment up or down based on stress contrast) with a limited number of  $0^\circ$  or  $180^\circ$  phased perforations.

Arguments are made for and against underbalanced vs. overbalanced perforating: underbalanced perforating may cause formation failure and cause the guns to “stick,” while overbalanced perforating eliminates a cleanup trip but may negatively impact the completion efficiency.

Solvent or other scouring pills are commonly circulated to the bottom of the workstring and then reversed out to remove scale, pipe dope, or other contaminants before they are pumped into the formation. Several hundred gallons (10 to 25 gal/ft) of 10 to 15% HCl acid will then typically be circulated or bullheaded down to the perforations and be allowed to soak, (to improve communication with the reservoir by cleaning up the perforations and dissolving debris in the perforation tunnel). Some operators are beginning to forego the solvent and acid cleanup (obviously to reduce rig time and associated costs) from the perspective that, in HPF, the damaging material is pumped deep into the formation and will not seriously impact well performance.

##### 19-4.2 Mechanical Considerations

The vast majority of HPF treatments have been performed with the mechanical sand-control equipment in place. However, in some early jobs, the tip-screenout and gravel pack were done in two steps separated by a clean-out trip. Concerns with fluid loss/damage to the fracture and a desire to eliminate all unnecessary expense eventually discouraged this two-step approach. More recently, there is a trend toward screenless HPFs as described in Section 19-8.1.

Early treatments were plagued by rate and erosion-resistance limitations of the gravel-pack tools. Enlarged crossover ports have now been incorporated in the gravel-pack tools of all the major service companies, which minimize friction and erosion problems and allow for very aggressive treatment designs. The aggressive pumping schedules, in turn, have given rise to another problem: Tiner *et al.* (1996) report several instances where the blank liner above the screen has been collapsed at screenout. They suggest that the pressure outside the blank rises quicker than the internal pressure, resulting in a collapse of this “weak link.” The suggested remedy is the use of P-110 grade pipe for the blank.

Limitations were also evident in the surface equipment used on early treatments. The tendency was to approach these treatments (especially offshore) as an oversized gravel-pack operation. While HPF volumes are relatively

small for a fracture treatment, the high rates (20 bbl/min is common) and high proppant concentrations (up to 16 or 18 lb/gal) require high horsepower. Undersized gravel-pack units were often used in early jobs; otherwise, miscellaneous onshore fracturing units were hobbled together and placed on barges. This practice resulted in many failed treatments. Today, dedicated skid-mount units with fixed manifolds are widely available and provide adequate horsepower (including standby) within stringent space and weight limitations. Reliable mixing and blending equipment is now available to achieve the various fluid and additive specifications of HPF, including very-low to very-high proppant concentrations and slurry rates. Other than these considerations, the surface equipment is common to that used in conventional MHF operations.

### 19-4.3 Pretreatment Diagnostic Tests

The objective of pretreatment diagnostic tests (referred to as fracture calibration tests, minifrac, datafrac, etc.) is to determine within engineering bounds, the value of various parameters that govern the fracturing process. Fracture closure pressure (considered in most cases as equivalent to the minimum horizontal in-situ stress) and the fluid leakoff coefficient (used to describe bulk leakoff behavior) are the most common targets and are especially important in HPF as discussed previously. However, other information may also be sought or inferred, such as (1) fracture extension or propagation pressure (often referred to as formation parting pressure or FPP), (2) potential perforation or near-wellbore friction, (3) evidence of fracture-height containment, and (4) reservoir permeability.

Several features unique to high-permeability fracturing make well-specific design strategies highly desirable if not essential: (1) fracture design in soft formations is very sensitive to leakoff and net pressure, (2) the controlled nature of the sequential tip-screenout/fracture inflation and packing/gravel-packing process demands relatively precise execution strategies, and (3) the treatments are very small and typically “one-shot” opportunities. Furthermore, methods used in hard-rock fracturing for determining critical fracture parameters *a priori* (geologic models, log and core data or Poisson’s ratio computational models based on poroelasticity) are of limited value or not yet adapted to the unconsolidated, soft, high-permeability formations.

The preceding discussion of advanced leakoff models and their applicability to pressure falloff analysis not-

withstanding, three tests (with variations) form the current basis of pretreatment testing in high-permeability formations: step-rate tests, minifrac tests, and pressure falloff tests.

#### 19-4.3.1 Step-Rate Tests

The step-rate test (SRT), as implied by its name, involves injecting clean gel at several stabilized rates, beginning at matrix rates and progressing to rates above fracture extension pressure. In a high-permeability environment, a test may be conducted at rate steps of 0.5, 1, 2, 4, 8, 10, and 12 bbl/min, and then at the maximum attainable rate. The injection is held steady at each rate step for a uniform time interval, typically 2 or 3 min at each step.

In principle, SRTs are intended to identify the fracture extension pressure and rate. The stabilized pressure (ideally bottomhole pressure) at each step is classically plotted on a Cartesian graph vs. injection rate. The point at which a straight line drawn through those points that are obviously below the fracture extension pressure (dramatic increase in bottomhole pressure with increasing rate) intersects with the straight line drawn through those points above the fracture extension pressure (minimal increase in pressure with increasing rate) is interpreted as the fracture extension pressure. The dashed lines on Figure 19-7 illustrate this classic approach.

While the conventional SRT is operationally simple and inexpensive, it is not necessarily accurate. A Cartesian plot of bottomhole pressure versus injection rate, in fact, does not generally form a straight line for radial flow in an unfractured well. Simple pressure transient analysis of SRT data through the use of de-superposition techniques shows that *with no fracturing*, the pressure vs. rate curve should exhibit upward concavity.

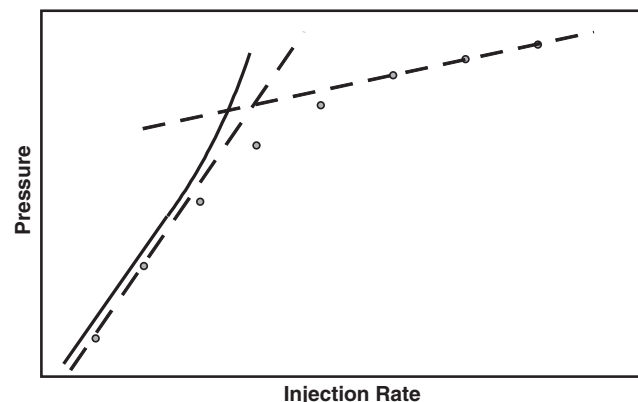


Figure 19-7 Ideal SRT—radial flow with no fracturing

Thus, the departure of the real data from ideal behavior may occur at a pressure and rate well below that indicated by the classic intersection of the straight lines (Figure 19-7).

The two-SRT procedure of Singh and Agarwal (1988) is more fundamentally sound. However, given the relatively crude objectives of the SRT in high-permeability fracturing, the conventional test procedure and analysis may be sufficient.

The classic test does indicate several things:

- Upper limit for fracture-closure pressure (useful in analysis of minifrac pressure falloff data)
- Surface treating pressure that must be sustained during fracturing (or whether sustained fracturing is even possible with a given fluid)
- Reduced rates that will ensure no additional fracture extension and (aided by fluid leakoff) packing of the fracture and near-wellbore with proppant
- Perforation and/or near-wellbore friction (indicated by bottomhole pressures that continuously increase with increasing rate, seldom a problem in soft formations with large perforations and high shot-densities)
- Expected casing pressure if the treatment is pumped with the service tool in the circulating position

A step-down option to the normal SRT is sometimes used specifically to identify near-wellbore restrictions (tortuosity or perforation friction). This test is usually done immediately following a minifrac pump-in stage. By observing how bottomhole pressure varies with decreasing rate, near-wellbore restrictions can be immediately detected; for example, bottomhole pressures that change only gradually during steps down in injection rate would indicate *no restriction*.

#### 19-4.3.2 Minifrac Tests

Following the SRT, which establishes the fracture extension pressure and places an upper bound on fracture closure pressure, a minifrac is typically performed to tailor or redesign the HPF treatment with well-specific information. This test is the critical pretreatment diagnostic test. The minifrac analysis and treatment redesign is now commonly done on site in less than an hour, or 2 to 3 hours at the most.

Concurrent with the rise of HPF, minifrac tests and especially the use of bottomhole pressure information have become much more common. Otherwise, the classic

minifrac procedure and primary outputs as described in Chapter 17 (fracture closure pressure and a single leakoff coefficient) are widely applied to HPF—this in spite of some rather obvious shortcomings.

The first step in analyzing a minifrac is determining fracture closure pressure, which is typically done by plotting the pressure decline after shut-in vs. some function of time. The main plots used to identify fracture closure are

- $p_{\text{shut-in}}$  vs.  $t$
- $p_{\text{shut-in}}$  vs.  $\sqrt{t}$
- $p_{\text{shut-in}}$  vs.  $g$ -function (and variations)
- $\log(p_{\text{ISIP}} - p_{\text{shut-in}})$

The selection of closure pressure using these plots, a difficult enough task in hard-rock fracturing, has proved to be arbitrary or nearly impossible in high-permeability, high fluid-loss formations. In some cases, the duration of the closure period is so limited (1 minute or less) that the pressure signal is masked by transient phenomena. Deviated wellbores and laminated formations (common in offshore U.S. Gulf Coast completions), multiple fracture closures, and other complex features are often evident during the pressure falloff. The softness (low elastic modulus) of these formations results in very subtle fracture closure signatures on the pressure decline curve. Flowbacks are not used to accent closure features because of the high leakoff and concerns with production of unconsolidated formation sand.

New guidelines and diagnostic plots for determining closure pressure in high-permeability formations are being pursued by various practitioners, and this information will eventually emerge to complement or replace the standard analysis and plots.

The shortcomings of classic minifrac analysis are further exposed when they are used (commonly) to select a single effective fluid-loss coefficient for the treatment. As described in Chapter 17, in low-permeability formations, this approach results in a slight overestimation of fluid loss and actually provides a factor of safety to prevent screenout. In high-permeability formations, the classic approach can dramatically underestimate spurt loss (zero spurt-loss assumption) and overestimate total fluid loss (Dusterhoft *et al.*, 1995). This uncertainty in leakoff behavior makes the controlled timing of a tip-screenout very difficult. Dusterhoft *et al.* outlined various procedures to correct for spurt loss and leakoff behavior that is not proportional to the square root of time; however,

entirely new procedures based on sound fundamentals of leakoff in HPF (as outlined previously in Section 19-3.3) are ultimately needed. The traditional practice of accounting for leakoff with a bulk leakoff coefficient is simply not sufficient for this application.

#### 19-4.3.3 Pressure Falloff Tests

A third class of pretreatment diagnostics for HPF has emerged that is *not* common to MHF: pressure falloff tests. Because of the high formation permeability, common availability of high-quality bottomhole pressure data and multiple pumping and shut-in cycles, matrix formation properties including  $kh$  and skin can be determined from short-duration pressure falloff tests with the appropriate transient flow equation. Chapman *et al.* (1996) and Barree *et al.* (1996) propose prefrac or matrix injection/falloff tests that involve injecting completion fluid below fracturing rates for a given period, and then analyzing the pressure decline with a Horner plot. The test is performed with standard pumping equipment, and it poses little interruption to normal operations. A test can normally be completed within 1 hour or may even make use of data from unplanned injection/shut-in cycles. The resulting permeability certainly relates to fluid leakoff as described earlier in this chapter (Section 19-3.3.2), and it allows the engineer to better anticipate fluid requirements. An initial skin value is useful in “benchmarking” the HPF treatment and for comparison with post-treatment pressure transient analysis.

#### 19-4.3.4 Bottomhole Pressure Measurements

A discussion of pretreatment diagnostic tests requires a discussion of the source of pressures used in the analysis. Implicit to the discussion is that the only meaningful pressures are those adjacent to the fracture face, whether measured directly or translated to that point. At least four different types of bottomhole pressure data are available, depending on the location at which the real data were taken:

- Calculated bottomhole pressure (bottomhole pressure calculated from surface pumping pressure)
- Deadstring pressure (open annulus and bottomhole pressure determined based on the density of fluid in annulus; tubing may also be used as a deadstring when the treatment is pumped down the casing)
- Bundle carriers in the workstring (measured downhole, but above the service tool crossover)
- Washpipe data (from sensors attached to washpipe below the service-tool crossover)

Washpipe pressure data is the most desirable for HPF design and analysis because of its location adjacent to the fracture and downstream of all significant flowing pressure drops. Workstring bundle carrier data can introduce serious error in many cases because of fluid friction generated both through the crossover tool and in the casing/screen annulus. Without detailed friction-pressure corrections that account for specific tool dimensions and annular clearance, significant differences may exist between washpipe and workstring bundle carrier pressures (Mullen *et al.*, 1994). Deadstring pressures are widely used and considered acceptable by most practitioners; others suggest that redundant washpipe pressure data has shown that the deadstring can miss subtle features of the treatment. The use of bottomhole transducers with real-time surface readouts is suggested in cases where a deadstring is not feasible or when such well conditions as transients may obscure important information. The calculation of bottomhole pressures from surface pumping pressure is not recommended in HPF. The combination of heavy sand-laden fluids, constantly changing proppant concentrations, very high pump rates, and short pump times makes the estimation of friction pressures nearly impossible.

#### 19-4.4 Tip-Screenout Design

The so-called tip-screenout or TSO design clearly differentiates high-permeability fracturing (HPF) from conventional massive hydraulic fracturing (MHF). While HPF introduces other identifiable differences, such as higher permeability, softer rock, smaller proppant volumes, etc., it is the tip-screenout which makes these fracturing treatments unique. Conventional treatments are designed to achieve TSO at the end of pumping. In high-permeability fracturing, the *fracture creation* stage that precedes TSO is followed by a *fracture inflation and packing* stage; this two-stage treatment gives rise to the vernacular *fracpack*. These conventional and HPF design concepts are illustrated and compared in [Figure 19-4](#).

Because of the rapid ascent of high-permeability fracturing, many engineers did not have (and still do not have) computer models that accommodate the TSO design. By definition (Nolte, 1986), conventional fracture design systems were formulated with TSO as the endpoint. A no-growth fracture inflation and packing stage had not been envisioned, never mind entering the necessary design algorithms into a computer model. Recently,

however, several of the commercially available simulators have been modified to accept the TSO designs. The in-house simulators of many producing companies and oilfield service companies have also been modified.

Given the near-crippling dependence of the modern petroleum engineer on “black-box” solutions, one is compelled to ask how engineers effected a TSO design before the modified computer programs were available. What is the key? An experienced engineer would recognize that after TSO (assuming complete arrest of fracture growth), the problem is reduced to a simple one of material balance.

Wong *et al.* (1995) offer the following algorithm that can be used with any conventional 2D simulator to develop a fundamentally sound tip-screenout design:

1. It is assumed that the following fracture parameters are known at the end of the TSO stage (from the simulator):

$A_0$  = fracture area at TSO  
 $t_0$  = total time to TSO  
 $M_{ts0}$  = total proppant mass  
 $p(t_0)$  = net pressure at TSO  
 $V_{F(t_0)}$  = fracture volume at TSO

2. For every  $i^{\text{th}}$  stage of the fracture inflation and packing (FIP) pumping schedule, the clean fluid volume ( $V_{ci}$ ) and the pumping time for the  $i^{\text{th}}$  stage ( $t_i$ ) are given in terms of known slurry volume ( $V_i$ ), proppant concentration ( $c_i$ ), pump rate ( $q_i$ ), and proppant specific density ( $\rho_p$ ):

$$V_{ci} = V_i \rho_p / (\rho_p + c_i) \quad (19-8)$$

and

$$t_i = V_i / q_i \quad (19-9)$$

3. Cumulative time from TSO to the  $i^{\text{th}}$  stage is simply

$$T_i = \sum t_i \quad (19-10)$$

4. Assuming that the fracture area ceases to propagate after TSO, the fluid leakoff rate ( $q_l$ ) and leakoff volume ( $V_l$ ) at any time  $T_i$  are given (for low-efficiency conditions) as

$$q_l(T_i) = 2C_L A_0 (1/\sqrt{t_0}) \arcsin(1/\sqrt{\tau_i}) \quad (19-11)$$

and

$$V_l(T_i) = 2C_L A_0 \sqrt{t_0} \left[ \tau_i \arcsin(1/\tau_i) + \sqrt{\tau_i - 1} \right] \quad (19-12)$$

where

$$\tau_i = (t_0 + T_i) / t_0 \quad (19-13)$$

and  $C_L$  is the fluid leakoff coefficient.

5. The following material balance relations can be easily implemented in a spreadsheet program and used to calculate fracture parameters at any time  $T_i$ :

$$V_f(T_i) = \sum V_{ci} - V_l(T_i) \quad (19-14)$$

$$V_f(T_i) = V_F(t_0) + \sum V_i - V_l(T_i) \quad (19-15)$$

$$M_{fip}(T_i) = M_{ts0} + \sum (c_i V_{ci}) \quad (19-16)$$

$$c_m(T_i) = M_{fip}(T_i) / V_f(T_i) \quad (19-17)$$

$$APC(T_i) = M_{fip}(T_i) / A_0 \quad (19-18)$$

and

$$\Delta p(T_i) = \Delta p(t_0) \frac{V_F(T_i)}{V_F(t_0)} \quad (19-19)$$

where  $V_f$  is the total (two-wing) fluid volume,  $V_F$  is the total fracture volume,  $M_{fip}$  is the total amount of proppant,  $c_m$  is the average proppant concentration loading,  $APC$  is the average areal proppant concentration, and  $\Delta p$  is the net pressure.

Using the relations above, a TSO design is developed that specifies pump rate, slurry volume, and proppant loading during fracture inflation and packing in as many stages as deemed appropriate. Design objectives include (1) achieving a desired fracture width (from areal proppant concentration) and (2) ensuring that the proppant does not dehydrate prematurely ( $c_m < 28$  lb/gal).

Early TSO treatment designs commonly called for 50% pad (similar to conventional fracturing) and a fairly aggressive proppant ramping schedule; however, it is now increasingly common to reduce the pad to 10 to

15% of the treatment and extend the 0.5 to 2 lb/gal stages (which combined, may comprise 50% of total slurry volume, for example). This practice is intended to “create width” for the higher concentration proppant addition (12 to 14 lb/gal).

### 19-4.5 Pumping a TSO Treatment

Anecdotal observations related to real-time HPF experiences are abundant in the literature and are not the focus of this text. However, some observations related to treatment execution are necessary:

- Most treatments are pumped with a gravel-pack service tool in the “circulate” position with the annulus valve closed at the surface. This practice allows for live annulus monitoring of bottomhole pressure (annulus pressure + annulus hydrostatic head) and real-time monitoring of the progress of the treatment.
- When no evidence exists of the planned TSO on the real-time pressure record, the late treatment stages can be pumped at a reduced rate to effect a tip-screenout. Obviously, this practice requires reliable bottomhole pressure data and direct communication with the frac unit operator.
- Near the end of the treatment, the pump rate can be slowed to gravel-packing rates, and the annulus valve can be opened to begin circulating a gravel pack. The reduced pump rate is maintained until tubing pressure reaches a safe upper limit, signaling that the screen/casing annulus is packed.
- Because very high proppant concentrations are used, the sand-laden slurry used to pack the screen/casing annulus must be displaced from the surface with clean gel well before the end of pumping. Thus, proppant addition and slurry volumes must be metered carefully to ensure that there is sufficient proppant left in the tubing to place the gravel pack (to avoid “overdisplacing” proppant into the fracture).
- Conversely, if an HPF treatment sands out prematurely (with proppant in the tubing), the service tool can be moved into the “reverse” position and the excess proppant can be circulated out.
- Movement of the service tool from the squeeze/circulating position to the reverse position can create a sharp instantaneous drawdown effect, and it should be done carefully to avoid swabbing unstabilized for-

mation material into the perforation tunnels and annulus.

#### 19-4.5.1 Swab Effect Example

The following simple equation, given by Mullen *et al.* (1994) can be used to convert swab volumes into oil-field-unit flow rates.

$$q_s = 2057 \frac{V_s}{t_m} \quad (19-20)$$

where  $q_s$  is the instantaneous swab rate in bbl/d,  $V_s$  is the swabbed volume of fluid in gal,  $t_m$  is the time of tool movement in seconds, 2057 is the conversion factor for gal/sec to bbl/d.

The volume of swabbed fluid is calculated from the service-tool diameter and the length of stroke during which the sealed service tool does not allow fluid bypass. The average swab volume of a 2.68-in. service tool is 2.8 gal when the service tool is moved from the squeeze position to the reverse-circulation position. Assuming a rather normal movement time of 5 seconds, this represents an instantaneous production rate of 1103 bbl/d.

## 19-5 FRACTURE CONDUCTIVITY AND MATERIALS SELECTION

### 19-5.1 Optimum Fracture Dimensions

Much has been published recently concerning optimum fracture dimensions in HPF. While there are debates regarding the optimum dimensions, fracture conductivity is largely regarded as more important than fracture length. Of course, this intuitive statement only recognizes the first principle of fracture optimization: Higher permeability formations require higher fracture conductivity to maintain an acceptable value of the dimensionless fracture conductivity,  $C_{FD}$ .

So how long should the fracture be? A “rule of thumb” is that fracture length should be equal to half the perforation height (thickness of producing interval). Alternatively, Hunt *et al.* (1994) showed that cumulative recovery from a well in a 100-md reservoir with a 10-ft damage radius is optimized by extending a fixed 8000-md-ft conductivity fracture to any appreciable distance beyond the damaged zone. This result implies that there is little benefit to a 50-ft fracture length compared to a 10-ft fracture length. Two observations are in order: first, the Hunt *et al.* evaluation is based on cumulative

recovery; second, their assumption of a fixed fracture conductivity implies a decreasing dimensionless fracture conductivity with increasing fracture length (less than optimal placement of the proppant).

It is generally true that if an acceptable  $C_{fD}$  is maintained, additional length will provide additional production. (An acceptable  $C_{fD}$  may require an increase in areal proppant concentration from 1.5 lb/ft<sup>2</sup>, which is common in hard-rock fracturing, to 20 lb/ft<sup>2</sup> or more.) Ultimately, the decision becomes one of economics and/or optimal placement of a finite proppant volume (as in offshore environments where total fluid and proppant volumes may be physically limited).

These issues are discussed more rigorously in the following sections.

### 19-5.1.1 Fracture Width as a Design Variable

In practice, fracture extent and width have been difficult to influence separately. Once a fracturing fluid and injection rate are selected, the fracture width evolves with increasing length according to strict relations (at least in the well-known PKN and KGD design models). Therefore, the key decision variable has been the fracture extent. Once a fracture extent is selected, the width is calculated as a consequence of technical limitations, (maximum realizable proppant concentration). Knowledge of the leakoff process helps to determine the necessary pumping time and pad volume.

The tip-screenout (TSO) technique has brought a significant change to this design philosophy. Through TSO, fracture width can be increased without increasing the fracture extent. In this context, a strictly technical optimization problem can be formulated: How does one independently select the optimum fracture length and width under a given proppant volume constraint? The problem is one of maximizing the PI in the pseudosteady-state flow regime. The answer is of primary importance in understanding HPF, but is also necessary for understanding hydraulic fracturing in general.

The same propped volume can be used to create a narrow, elongated fracture or a wide, short fracture. It is convenient to select  $C_{fD}$  as the decision variable, and then the fracture half-length can be expressed using the propped volume of one wing,  $V_f$ , as

$$x_f = \left( \frac{V_f k_f}{C_{fD} h k} \right)^{1/2} \quad (17-9)$$

The productivity index (Equation 19-1) after the creation of a fracture of half-length,  $x_f$ , can be written in oilfield units as

$$J = \frac{kh}{141.2B\mu \left[ \ln \frac{0.472r_e}{r_w} + \ln \frac{r_w}{x_f} + \left( \ln \frac{x_f}{r_w} + s_f \right) \right]} \quad (19-21)$$

where  $s_f$  is the Cinco-Ley *et al.* pseudoskin appearing because of the fracture. The quantity  $\ln x_f/r_w + s_f$  can be obtained from the dimensionless fracture conductivity,  $C_{fD}$ , (Equation 17-8). The wellbore radius drops out and the fracture half-length is substituted from Equation 17-9. The resulting productivity index is

$$J = \frac{kh}{141.2B\mu \left[ \ln 0.472r_e + 0.5 \ln \frac{hk}{V_f k_f} + 0.51 \ln C_{fD} + \left( \ln \frac{x_f}{r_w} + s_f \right) \right]} \quad (19-22)$$

where the only unknown is  $C_{fD}$ . Since the drainage radius, formation thickness, two permeabilities, and the propped volume are fixed, the maximum PI occurs when the quantity

$$y = 0.51 \ln C_{fD} + \ln \frac{x_f}{r_w} + s_f \quad (19-23)$$

becomes a minimum. The quantity  $y$  is also shown on Figure 19-2. Since it depends only on  $C_{fD}$ , the optimum  $C_{fD, \text{opt}} = 1.6$  is a *given constant* for any reservoir, well, and proppant. (Note: Depending on the accuracy of the calculations and the graphical representation, some authors have suggested the value 1.2.) As explained in Chapter 17, the optimum dimensionless fracture conductivity corresponds to the best compromise between the capacity of the fracture to conduct and the capacity of the reservoir to deliver hydrocarbon.

### 19-5.1.2 Technical Optimization

Once the volume of proppant that can be placed into one wing of the fracture,  $V_f$ , is known, the optimum fracture half-length can be calculated as

$$x_f = \left( \frac{V_f k_f}{1.6hk} \right)^{1/2} \quad (19-24)$$

and consequently, the optimum propped average width should be

$$w = \left( \frac{1.6V_f k}{hk_f} \right)^{1/2} \quad (19-25)$$

These results have several implications. Most important, there is no theoretical difference between low- and high-permeability fracturing. In both cases, a *technically* optimal fracture exists, and it should have a dimensionless fracture conductivity of order unity. In a low-permeability formation, this requirement results in a long and narrow fracture. In high-permeability formations, a short and wide fracture may provide the same dimensionless conductivity. In practice, not all proppant will be placed into the permeable layer, so in the relation above, the *effective* volume should be used, subtracting the proppant placed in the nonproductive layers. It is also important to recognize that the indicated “optimal fracture” may not always be feasible. In high-permeability formations, departure from the optimum dimensionless fracture conductivity might be justified by several factors (e.g. the indicated large width may be impossible to create): a minimum length may be dictated by the damage radius, severe non-Darcy effects in the fracture may strongly reduce the apparent permeability of the proppant pack, and considerable fracture width can be lost because of proppant embedment into the soft formation.

### 19-5.1.3 Economic Optimization

Having settled the optimization of fracture length vs. width for a fixed proppant volume, the remaining task is to optimize proppant volume. Obviously, this is an economic optimization issue rather than a technical one. The more proppant that is placed in the formation (otherwise optimally), the better the performance of the well. At this point, economic considerations must dominate. The additional revenue at some point becomes marginal compared to the linearly (or even more strongly) increasing costs. This situation is properly treated by applying net present value (NPV) analysis (Balen *et al.*, 1988). Though a NPV analysis always provides an “optimum design,” it should not replace the understanding of the underlying technical optimization issues.

## 19-5.2 Proppant Selection

The primary and unique issue relating to proppant selection for high-permeability fracturing is *proppant sizing*. Proppant strength, shape, composition, and other factors are included in a more general discussion of proppant

selection in Section 17-3.4. Resin-coated proppants are discussed briefly as an emerging HPF technology in Section 19-8.1. While specialty proppants (intermediate-strength and resin-coated proppants) have certainly been used in HPF, most treatments are pumped with standard graded-mesh sand.

When selecting a proppant size for HPF, the engineer faces competing priorities: sizing the proppant to address concerns with sand exclusion, or using maximum proppant size to ensure adequate fracture conductivity.

As with equipment choices and fluids selection, the gravel-packing roots of fracpack are also evident when proppant selection is considered. Engineers initially focused on sand exclusion and a gravel pack derived sizing criteria such as that proposed by Saucier (1974). Saucier recommends that the mean gravel size ( $D_{g50}$ ) be five to six times the mean formation grain size ( $D_{f50}$ ). The so-called “4-by-8 rule” represents minimum and maximum grain-size diameters that are distributed around Saucier’s criteria, i.e.  $D_{g,\min} = 4D_{g50}$  and  $D_{g,\max} = 8D_{g50}$ , respectively. Thus, many early treatments were pumped with standard 40/60-mesh or even 50/70-mesh sand. The somewhat limited conductivity of these gravel-pack mesh sizes under in-situ formation stresses may not be adequate in many cases. Irrespective of sand mesh size, fracpacks tend to reduce concerns with fines migration by reducing fluid flux at the formation face.

The current trend in proppant selection is to use fracturing-size sand. A typical HPF treatment now uses 20/40 proppant (sand). Maximizing the fracture conductivity can itself help prevent sand production by reducing drawdown. Results with the larger proppant have been encouraging, both in terms of productivity and limiting or eliminating sand production (Hannah *et al.*, 1993).

It is interesting to note that the topics of formation competence and sanding tendency, major issues in the realm of gravel-pack technology, have not been widely studied in the context of HPF. In many cases, HPF is providing a viable solution to completion failures *despite* the industry’s limited understanding of (soft) rock mechanics.

This move away from gravel-pack practices toward fracturing practices is common to many aspects of HPF with the exception (so far) of downhole tools, and it seems to justify changing our terminology from *fracpack* to *high-permeability fracturing*. The following discussion of fluid selection is also consistent with this perspective.

### 19-5.3 Fluid Selection

Fluid selection for HPF has always been driven by concerns with damaging the high-permeability formation, either by filter-cake buildup or (especially) polymer invasion. Most early treatments were performed with HEC, the classic gravel-pack fluid, because it was perceived to be less damaging than guar-based fracturing fluids. While the debate continues and many operators continue to use HEC fluids, the fluid of choice is increasingly borate-crosslinked HPG.

Based on a synthesis of reported findings from several practitioners, Aggour and Economides (1996) provide a well-reasoned rationale to guide fluid selection in HPF. Their findings suggest that if the extent of fracturing fluid invasion is minimized, the degree of damage (permeability impairment caused by filter-cake or polymer invasion) is of secondary importance. They use the effective skin representation of Mathur *et al.* (1995) to show that if fluid leakoff penetration is small, even severe permeability impairments can be tolerated without exhibiting positive skin effects. In this case, the obvious recommendation in HPF is to use high-polymer concentration, crosslinked fracturing fluids with fluid-loss additives, and an aggressive breaker schedule. The polymer, crosslinker, and fluid-loss additives limit polymer invasion, and the breaker ensures maximum fracture conductivity, a critical factor which cannot be overlooked. Experimental work corroborates these contentions.

Linear gels have been known to penetrate cores of very low permeability (1 md or less) whereas crosslinked polymers are likely to build filter cakes at permeabilities two orders of magnitude higher (Roodhart, 1985; Mayerhofer *et al.*, 1991). Filter cakes, while they may damage the fracture face, clearly reduce the extent of polymer penetration into the reservoir that is normal to the fracture face. At extremely high permeabilities, even crosslinked polymer solutions may invade the formation.

Cinco-Ley and Samaniego (1981) and Cinco-Ley *et al.* (1978) described the performance of finite-conductivity fractures and delineated the following three major types of damage affecting this performance:

- *Reduction of proppant-pack permeability* resulting from either proppant crushing or (especially) unbroken polymer chains, leads to fracture conductivity impairment. This condition can be particularly problematic in moderate- to high-permeability reservoirs. Extensive progress in breaker technology has dramatically reduced concerns with this type of damage.

- *Choke damage* refers to the near-well zone of the fracture that can be accounted for by a skin effect. This damage can result from either overdisplacement at the end of a treatment or by fines migration (native or proppant) during production and the accumulation of fines near the well but within the fracture.
- *Fracture-face damage* implies permeability reduction normal to the fracture face and includes permeability impairments caused by the filter cake, polymer-invaded zone, and filter cake-invaded zone.

#### 19-5.3.1 Composite Skin Effect

Mathur *et al.* (1995) provide the following representation for effective skin resulting from radial wellbore damage and fracture-face damage:

$$s_d = \frac{\pi}{2} \left[ \frac{b_2 k_r}{b_1 k_3 + (x_f - b_1) k_2} + \frac{(b_1 - b_2) k_r}{b_1 k_1 + (x_f - b_1) k_r} - \frac{b_1}{x_f} \right] \quad (19-26)$$

Figure 19-8 depicts the two types of damage accounted for in  $s_d$ , (fracture-face and radial wellbore damage). The  $b$ - and  $k$ - terms are defined graphically in Figure 19-9 and represent the dimensions and permeabilities of various zones included in the finite-conductivity fracture model of Mathur *et al.*

The equivalent damage skin from Equation 19-26 can be added directly to the undamaged fracture skin effect to obtain the total skin:

$$s_t = s_d + s_f \quad (19-27)$$

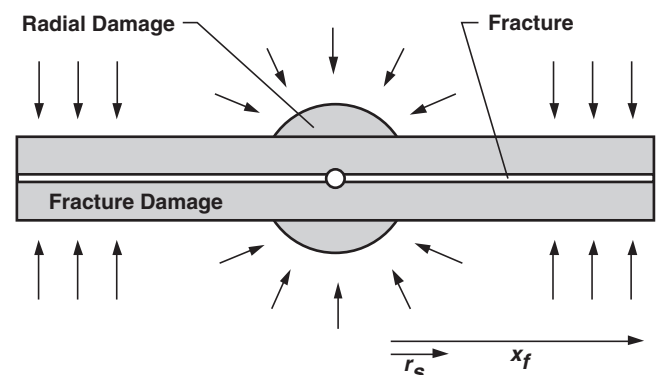


Figure 19-8 Fracture-face damage

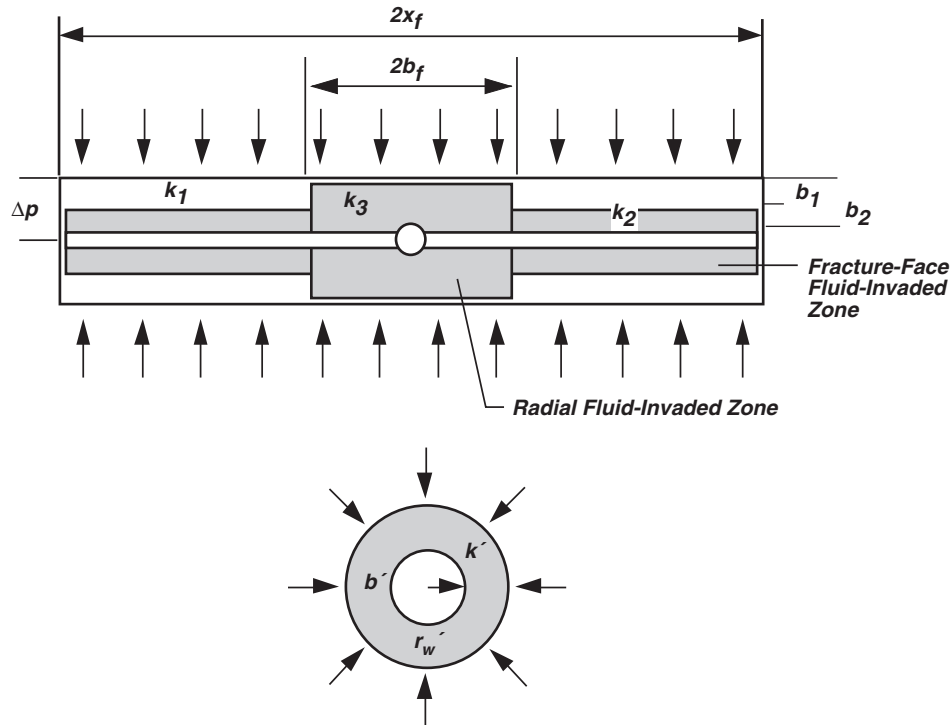


Figure 19-9 Fluid-invaded zones

### 19-5.3.2 Parametric Studies

Aggour and Economides (1996) used the Mathur *et al.* model (with no radial wellbore damage) to evaluate total skin and investigate the relative effects of different variables. Their results related the total skin in a number of discrete cases to (1) the depth of fluid invasion normal to the fracture face and (2) the degree of permeability reduction in the fluid-invaded zone. A sample of their results (for  $x_f = 25$  ft,  $C_{fD} = 0.1$ , and  $k_f = 10$  md), expressed initially in terms of damage penetration ratios,  $b_2/x_f$ , and permeability impairment ratios,  $k_2/k_r$ , are re-expressed in real units on Table 19-4. Under each of these conditions, the total skin is equal to zero.

These results suggest that for a (nearly impossible) 2.5-ft penetration of damage, a positive skin is obtained only if the permeability impairment in the invaded zone is

more than 90%. For 1.25-ft damage penetration, the permeability impairment would have to be over 95% to achieve positive skins. If the penetration of damage can be limited to 0.25 ft, even a 99% permeability reduction in the invaded zone would not result in positive skins. At a higher dimensionless conductivity equal to unity, even higher permeability impairments can be tolerated without suffering positive skins.

At least one obvious critical conclusion can be made from this work: The extent of damage normal to the fracture face is more important than the degree of damage. If fluid invasion can be minimized, even 99% damage can be tolerated. The importance of maximizing  $C_{fD}$  is also illustrated; certainly, a good proppant-pack should not be sacrificed in an attempt to minimize the fracture-face damage.

This conclusion emphasizes the selection of appropriate fracturing fluids:

- Linear gels because of their considerable leakoff penetration, are *not* recommended
- Crosslinked polymer fluids with high gel loadings appear to be much more appropriate
- Aggressive breaker schedules are imperative

Table 19-4 Total skin

Depth of Fluid Invasion	Permeability Reduction
2.5 ft	90%
1.25 ft	95%
0.25 ft	99%

After Aggour and Economides (1996)

- Filter-cake building additives may also be considered to minimize the spurt loss and total leakoff

### 19-5.3.3 Predicted Well Performance with Cleanup

Fracture-face damage should not significantly alter long-term HPF performance. Previous work has confirmed this conclusion. Mathur *et al.* (1995) used a case study from the Gulf Coast and Ning *et al.* (1995) studied gas wells in Alberta, Canada. The Mathur *et al.* study assumed a linear cleanup of the fracture and observed an early-time improvement of the production rate. The Ning *et al.* study showed that the effect of fracture conductivity on the long-term production rate was the significant factor, whereas the effects of fracture-fluid invasion damage were minimal.

### 19-5.3.4 Experiments in Fracturing Fluid Penetration

McGowen *et al.* (1993) presented a series of experiments showing the extent of fracturing fluid penetration in cores of various permeabilities. Fracturing fluids used were 70-lb/Mgal HEC and 30- or 40-lb/Mgal borate-crosslinked HPG. Filtrate volumes were measured in mL/cm<sup>2</sup> of leakoff area (centimeters of penetration) for a 10-md limestone and 200- and 1,000-md sandstones at 120°F and 180°F.

Several conclusions are drawn from this work:

- Crosslinked fracturing fluids are far superior to linear gels in controlling fluid leakoff. For example, 40-lb/Mgal borate-crosslinked HPG greatly outperforms 70-lb/Mgal HEC in a 200-md core at 180°F.
- Linear gel performs satisfactorily in 10-md rock but fails dramatically at 200 md. Even aggressive use of fluid-loss additives (40-lb/Mgal silica flour) does not appreciably alter the leakoff performance of HEC in a 200-md core.
- Increasing crosslinked gel concentrations from 30- to 40-lb/Mgal has a major impact on reducing leakoff in 200-md core. Crosslinked borate maintains excellent fluid-loss control in 200-md sandstone and performs satisfactorily even at 1000 md.

This experimental work strongly corroborates the modeling results of Aggour and Economides (1996) and suggests the use of higher-concentration crosslinked polymer

fluids with, of course, an appropriately designed breaker system.

### 19-5.3.5 Viscoelastic Carrier Fluids

HEC and borate-crosslinked HPG fluids are the dominant fluids currently used in HPF; however, a third class of fluid deserves to be mentioned, so-called viscoelastic surfactant (VES) fluids. There is little debate that these fluids exhibit excellent rheological properties and are nondamaging, even in high-permeability formations. The advantage of VES fluids is that they do not require the use of chemical breaker additives; the viscosity of this fluid conveniently breaks (leaving considerably less residue than polymer-based fluids) either when it contacts formation oil or condensate, or when its salt concentration is reduced. Brown *et al.* (1996) present typical VES fluid performance data and case histories.

The vulnerability of VES fluids is in their temperature limitations. The maximum application temperature for VES fluids has only recently been extended from 130°F to 200°F.

## 19-5.4 Quality Control

Many early HPF treatments failed because of equipment problems and a lack of quality control on fluids and proppants. In general, the intense quality control that is standard for onshore massive hydraulic fracture treatments was not immediately adopted on small offshore fracpack treatments. This invited skepticism of the merits of the process and somewhat slowed the introduction of HPF technology. In addition to quality-control procedures that have been instituted by all major service companies, it is now common for producing companies to supply a consultant or in-house specialist to oversee the quality control on most HPF treatments.

A number of control checks should be performed before each HPF treatment to verify the performance of all fluids and proppants. The treatment itself should also be closely monitored so that (1) to the extent possible, real-time modifications can be made that will improve the outcome of the treatment and (2) unavoidable deficiencies in the treatment execution can be appropriately evaluated *post-mortem*. The reader is referred to the *Stimulation Engineering Handbook* (Ely, 1994) for a detailed explanation of fracturing quality-control procedures.

## 19-6 EVALUATION OF HPF TREATMENTS: UNIFIED APPROACH

### 19-6.1 Production Results

The evaluation of HPF treatments can be viewed on several different levels. Economic justification (production results) is the first level on which HPF technology was (and continues to be) evaluated. Simply put, HPF has gained widespread acceptance because it allows operators to produce more oil at less cost.

McLarty and DeBonis (1995) report that fracpack treatments typically result in production increases 200 to 250% times that of comparable gravel packs, and offer the example cases in Table 19-5.

Similar reports of production increase are scattered throughout the body of HPF literature. Stewart *et al.* (1995) present a relatively comprehensive economic justification for HPF that considers (in addition to productivity improvements) the incremental cost of HPF treatments and the associated payouts, operating expenses, relative decline rates, and reserve recovery acceleration issues.

### 19-6.2 Evaluation of Real-Time Treatment Data

There is increasing recognition of the value of real-time HPF treatment data. Complete treatment records and digital treatment datasets are now routinely collected and evaluated as part of post-treatment analysis. In fact, a fracpack cooperative has been established at Texas A&M University to facilitate databanking of these real-time engineering datasets.

Treatment reconstruction and post-mortem diagnosis hold tremendous potential to improve HPF design and execution, but the usefulness of many ongoing efforts in this regard is limited. With the proliferation of user-friendly, “black box software,” many engineers embrace and increasingly confuse technology with computer software and simulations. A popular approach to evaluation

of real-time datasets (pretreatment and main treatment) is net-pressure history-matching, although this approach is not advocated.

The incorporation of multiple leakoff, stress, friction, and other variables in a 3D simulator, while it may (and invariably does) lead to an excellent “match,” unfortunately sacrifices the uniqueness (usefulness) of the evaluation by introducing multiple degrees of freedom. These activities may provide operators with qualitative direction on a case-by-case basis, but they also conceal the real issues and retard fundamental development of the technology.

In contrast to this approach, consider the step-wise approach for the evaluation of bottomhole treating pressures outlined by Valkó *et al.* (1996):

- A leakoff coefficient is determined from an evaluation of minifrac data using a minimum number of assumptions, minimum input data, and minimum user interaction. Radial fracture geometry and a combined Nolte-Shlyapobersky method are suggested.
- When the obtained leakoff coefficient is used, an almost automatic procedure is suggested to estimate the created fracture dimensions and the areal proppant concentration from the bottomhole-pressure curve monitored during the execution of the HPF treatment. This procedure (termed “slopes analysis”) is further developed and expanded in Section 19-7 as a fundamental and potentially important building block for the evaluation of real-time HPF data.
- The obtained fracture dimensions and areal proppant concentration can be converted into an equivalent fracture extent and conductivity. The actual performance of the well is analyzed on the basis of well-test procedures, and these results are compared to the results of the slopes analysis.

Conducting the procedure above for a large number of treatments originating from various operators will result in a data bank that ultimately improves the predictability and outcome of HPF treatments.

At present, there seems to be a trend in the industry to support joint efforts and assist mutual exchange of information. The procedure above provides a coherent (though not exclusive) framework to compare HPF data from various sources through the use of a common, cost-effective evaluation methodology.

**Table 19-5** Example Production Results

Job Type	Before	After
New Well Comparison	460 bopd	1,216 bopd
Recompletion (oil)	1,300 bopd	2,200 bopd
Recompletion (gas)	3.8 MMcf/d	13.2 MMcf/d
Sand Failure	200 bopd	800 bopd

After McLarty and DeBonis (1995)

### 19-6.3 Post-Treatment Pressure-Transient Analysis

For post-treatment evaluation, temperature logs and various fracture-mapping techniques, such as triaxial borehole seismics and radioactive tracer mapping, have gained increasing importance. However, from the basis of future production, by far the most important evaluation is pressure transient analysis. While avoiding an exhaustive treatment of the subject, it is appropriate at this juncture to discuss several issues related to pressure-transient analysis in HPF wells, especially positive skin factors, which pose the largest challenge to treatment evaluation.

The performance of a vertically fractured well under pseudosteady-state flow conditions was investigated by McGuire and Sikora (1960) through the use of a physical analog (electric current). A similar study for gas wells was conducted by van Poolen *et al.* (1958). For the “unsteady-state” case, a whole series of works was initiated by Gringarten and Ramey (1974), and continued by Cinco-Ley *et al.* (1978) They clarified concepts of the infinite-conductivity fracture, uniform-flux fracture, and finite-conductivity fracture. From the formation perspective, double-porosity reservoirs, multi-layered reservoirs, and several different boundary geometries have been considered. The typical flow regimes (fracture linear, bilinear, pseudoradial) have been well documented in the literature. Deviations from ideality (non-Darcy effects) have also been considered.

Post-treatment pressure transient analysis for HPF wells starts with a log-log diagnostic plot that includes the pressure derivative. Once the different flow regimes are identified, specialized plots can be used to obtain the characteristics of the created fracture. In principle, fracture length and/or conductivity can be determined using the prior knowledge of permeability. For HPF, however, the relatively large arsenal of pressure-transient diagnostics and analysis for fractured wells has proven somewhat ineffective. Often, it is difficult to reveal the marked characteristics of an existing fracture on the diagnostic plot. In fact, the well often behaves similar to a slightly damaged, unstimulated well. An HPF treatment is often considered successful if a large positive skin of order +10 or more is decreased to the range of +1 to +4. These (still) positive skin factors create the largest challenge of treatment evaluation.

The obvious discrepancy between theory and practice has been attributed to several factors, some of which are well documented and understood and some others of which are still in the form of hypotheses:

- **Factors causing decrease of apparent permeability in the fracture** The most familiar factor that decreases the apparent permeability of the proppant pack, and therefore fracture conductivity, is *proppant-pack damage*. The reduction of permeability because of the presence of residue from the gelled fluid and failure of proppant because of closure stress are well understood. Since those phenomena exist in any fracture, they cannot be the general cause of the discrepancy in high-permeability fracturing. *Non-Darcy flow in the fracture* is also reasonably well understood. Separation of rate-independent skin from the variable-rate component by multiple-rate well testing is a standard practice. The effect of *phase change in the fracture* is less straightforward to quantify.
- **Factors decreasing the apparent width** Embedment of the proppant in a soft formation is now well documented in the literature (e.g. Lacy *et al.*, 1996).
- **Fracture-face skin effect** The two sources of this phenomenon are filter-cake residue and the polymer-invaded zone. Sometimes the long-term cleanup (decrease of the skin effect) of a stimulated well is considered as indirect proof of such damage. It is assumed that linear polymer fluids invade more deeply into the formation and therefore, cause more fracture-face damage, as discussed by Mathur *et al.* (1995).
- **Permeability anisotropy** While the anisotropy of permeability has only a limited effect on pseudoradial flow, the early-time transient flow regime of a stimulated well is very sensitive to anisotropy. This fact is often neglected when the well is characterized with one single skin effect.
- **Concept of skin** It has to be emphasized that the concept of negative skin as the only measure of the “quality” of a well might be a source of the discrepancy itself.

#### 19-6.3.1 Validity of the Skin Concept in HPF

There is, in fact, no clear theoretical base for obtaining negative skin from short-time well-test data distorted by wellbore storage if the well has been stimulated. The use of infinite-acting reservoir + wellbore storage + skin type-curves in this case is not based on sound physical principles and might cause unrealistic conclusions.

In addition, the validity of the pseudoskin concept during the transient production period is an important issue. In general, the pseudoskin concept is valid only at late times. Thus, a fracture designed for optimal late-time

performance may be not optimal at shorter times. One may ask how much performance is lost in selecting fracture dimensions that are optimal for a late time. This question has not been investigated, but it is reasonable to assume that the loss in performance is negligible for high-permeability reservoirs where the dimensionless times corresponding to a month or year are much higher than for low-permeability reservoirs.

### 19-6.3.2 Effect of Non-Darcy Flow in the Fracture

Non-Darcy flow is another important issue that deserves specific consideration in the context of HPF. Non-Darcy flow in gas reservoirs causes a reduction of the productivity index by at least two mechanisms. First, the apparent permeability of the formation may be reduced (Wattenbarger and Ramey, 1969) and second, the non-Darcy flow may decrease the conductivity of the fracture (Guppy *et al.*, 1982).

Consider a closed gas reservoir producing under pseudosteady-state conditions, and apply the concept of pseudoskin effect determined by dimensionless fracture conductivity.

#### Definitions and Assumptions

Gas production is calculated from the pseudosteady-state deliverability equation:

$$q = \frac{\pi khT_{sc} [m(\bar{p}) - m(p_{wf})]}{p_{sc} T} \times \frac{k_{r,app}}{k_r \left[ f_1(C_{fD,app}) + \ln \left( \frac{0.472r_e}{x_f} \right) \right]} \quad (19-28)$$

where  $m(p)$  is the pseudopressure function,  $k_{f,app}$  is the apparent permeability of the proppant in the fracture, and  $k_{r,app}$  is the apparent permeability of the formation. (All the equations in this subsection are given for a consistent system of units, such as SI.) The function  $f_1$  was introduced by Cinco-Ley and Samaniego (1981); it was presented in Chapter 17 as

$$f_1(C_{fD}) = s_f + \ln \frac{x_f}{r_w} = \frac{1.65 - 0.328u + 0.116u^2}{1 + 0.18 \ln u + 0.064u^2 + 0.005u^3} \quad (17-8)$$

where  $u = \ln C_{fD}$ .

The apparent dimensionless fracture conductivity is defined by

$$C_{fD,app} = \frac{k_{f,app} w}{k_{r,app} x_f} \quad (19-29)$$

The apparent permeabilities are flow-rate dependent; therefore, the deliverability equation becomes implicit in the production rate.

Proceeding further requires a model of non-Darcy flow. Almost exclusively, the Forcheimer equation is used in the industry:

$$-\frac{dp}{dx} = \frac{u}{k} v + \beta \rho |v| v \quad (19-30)$$

where  $v = q_a/A$  is the Darcy velocity and  $\beta$  is a property of the porous medium.

A popular correlation was presented by Firoozabadi and Katz (1979) as

$$\beta = \frac{c}{k^{1.2}} \quad (19-31)$$

where  $c = 8.4 \times 10^{-8} \text{ m}^{1.4}$  ( $= 2.6 \times 10^{10} \text{ ft}^{-1} \text{ md}^{1.2}$ ).

To apply the Firoozabadi and Katz correlation, we write

$$-\frac{dp}{dx} = \mu v \frac{1}{k} \left( 1 + \frac{\beta k \rho |v|}{\mu} \right) = \mu v \frac{1}{k} \left( 1 + \frac{c \rho |v|}{k^{0.2} \mu} \right) \quad (19-32)$$

showing that

$$\frac{k_{app}}{k} = \frac{1}{1 + \frac{c \rho |v|}{k^{0.2} \mu}} \quad (19-33)$$

The equation above can be used both for the reservoir and for the fracture if correct representative linear velocity is substituted. In the following, it is assumed that  $h = h_f$ .

A representative linear velocity for the reservoir can be given in terms of the gas-production rate as

$$v = \frac{q_a}{4hx_f} \quad (19-34)$$

where  $q_a$  is the in-situ (actual) volumetric flow rate; therefore, for the reservoir non-Darcy effect

$$\left( \frac{c \rho v}{k^{0.2} \mu} \right)_r = \left( \frac{c \rho q_a}{2h\mu} \right) \frac{1}{2x_f k_r^{0.2}} \quad (19-35)$$

A representative linear velocity in the fracture can be given in terms of the gas-production rate as

$$v = \frac{q_a}{2hw} \quad (19-36)$$

Thus, for the non-Darcy effect in the fracture, one can use

$$\left(\frac{c\rho v}{k^{0.2}\mu}\right)_f = \left(\frac{c\rho q_a}{2h\mu}\right) \frac{1}{wk_f^{0.2}} \quad (19-37)$$

The term  $\rho q_a$  is the mass flow rate, and it is the same in the reservoir and in the fracture;  $c\rho q_a$  is expressed in terms of the gas-production rate as

$$\frac{c\rho q_a}{2h\mu} = \frac{c\rho_a\gamma_g}{2h\mu} q = c_0 q \quad (19-38)$$

where  $q$  is the gas-production rate in standard volume per time,  $\gamma_g$  is the specific gravity of gas with respect to air, and  $\rho_a$  is the density of air at standard conditions. The factor  $c_0$  is constant for a given reservoir-fracture system.

The final form of the apparent permeability dependence on production rate is

$$\left(\frac{k_{\text{app}}}{k}\right)_r = \frac{1}{1 + \frac{c_0 q}{2x_f k_r^{0.2}}} \quad (19-39)$$

for the reservoir and

$$\left(\frac{k_{\text{app}}}{k}\right)_f = \frac{1}{1 + \frac{c_0 q}{wk_f^{0.2}}} \quad (19-40)$$

for the fracture. As a consequence, the deliverability equation becomes

$$q = \frac{\pi khT_{sc} [m(\bar{p}) - m(p_{wf})]}{p_{sc} T} \times \frac{1}{\left(1 + \frac{c_0 q}{2x_f k_r^{0.2}}\right) \left[ f_1(C_{fD,\text{app}}) + \ln\left(\frac{0.472r_e}{x_f}\right) \right]} \quad (19-41)$$

where

$$C_{fD,\text{app}} = \frac{k_f w}{k_r x_f} \frac{1 + \frac{c_0}{wk_f^{0.2}} q}{1 + \frac{c_0}{2x_f k_r^{0.2}} q} \quad (19-42)$$

The *additional* skin effect,  $s_{ND}$ , appearing because of non-Darcy flow, can be expressed as

$$s_{ND} = \left(1 + \frac{c_0 q}{2x_f k_r^{0.2}}\right) \left[ f_1(C_{fD,\text{app}}) + \ln\left(\frac{0.472r_e}{x_f}\right) \right] - \left[ f_1(C_{fD}) + \ln\left(\frac{0.472r_e}{x_f}\right) \right] \quad (19-43)$$

The additional non-Darcy skin effect is always positive and depends on the production rate in a nonlinear manner.

Equations 19-29 and 19-31 are of primary importance for interpreting post-fracture well-testing data and to forecast production. If the mechanism responsible for the post-treatment skin effect is not understood clearly, the evaluation of the treatment and the production forecast might be severely erroneous.

### 19-6.3.3 Case Study in Effect of Non-Darcy Flow

As discussed above, non-Darcy flow in a gas reservoir reduces the productivity index by at least two mechanisms. First, the apparent permeability of the formation may be reduced, and second, the non-Darcy flow may decrease the fracture conductivity. In this case study, the effect of non-Darcy flow on production rates and observed skin effects is investigated. Reservoir and fracture properties are given in Table 19-6.

A simplified form of Equation 19-41 in field units is

$$q = \frac{\bar{p}^2 - p_{wf}^2}{1424\mu ZT} \times \frac{1}{\left(1 + \frac{c_0 q}{2x_f k_r^{0.2}}\right) \left[ f_1(F_{CD,\text{app}}) + \ln\left(\frac{0.472r_e}{x_f}\right) \right]} \quad (19-44)$$

where  $c_0 = \frac{c\rho_a\gamma_g}{2h\mu}$  has to be expressed in ft-md<sup>0.2</sup> MMscf/d. In the given example,  $c_0 = 73$  ft-md<sup>0.2</sup> MMscf/d and

**Table 19-6.** Data for fractured well in gas reservoir

$r_e$	ft	1 500
$\mu$	cp	0.02
$Z$	N/A	0.95
$T$	$^{\circ}\text{R}$	640
$k_r$	md	10
$h$	ft	80
$h_f$	ft	80
$k_f$	md	10,000
$x_f$	ft	30
$w$	inch	0.5
$\gamma_g$	N/A	0.65
$\bar{p}$	psi	4 000
$r_w$	ft	0.328

$$C_{JD,app} = \left( \frac{k_f w}{k_r x_f} \right) \frac{1 + \frac{c_0}{2x_f k_r^{0.2}} q}{1 + \frac{c_0}{w k_f^{0.2}} q} = \left( \frac{k_f w}{k_r x_f} \right) \frac{1 + c_{0r} q}{1 + c_{0f} q} \tag{19-45}$$

where

$$c_{0r} = 2.34 \times 10^{-3} \text{ m}^3/\text{s} = 7.67 \times 10^{-2} (\text{Mscf/d})^{-1}$$

$$c_{0f} = 6.14 \times 10^{-1} \text{ m}^3/\text{s} = 2.78 \times 10^2 (\text{Mscf/d})^{-1}$$

Therefore, in field units

$$C_{JD,app} = 1.39 \frac{1 + 0.76q}{1 + 280q} \tag{19-46}$$

and

$$q = \frac{4000^2 - p_{wf}^2}{21.645} \times \frac{1}{(1 + 0.76q)[f_1(F_{CD,app}) + 3.16]} \tag{19-47}$$

The non-Darcy component of the skin effect can be calculated as

$$s_{ND} = (1 + 0.00076q)[f_1(F_{CD,app}) + 3.16] - 4.619 \tag{19-48}$$

The results are shown graphically in Figs. 19-10 through 19-12. It is apparent that the effect of the fracture (negative skin on the order of  $-3$ ) is hidden by the positive skin effect induced by non-Darcy flow. The zero or posi-

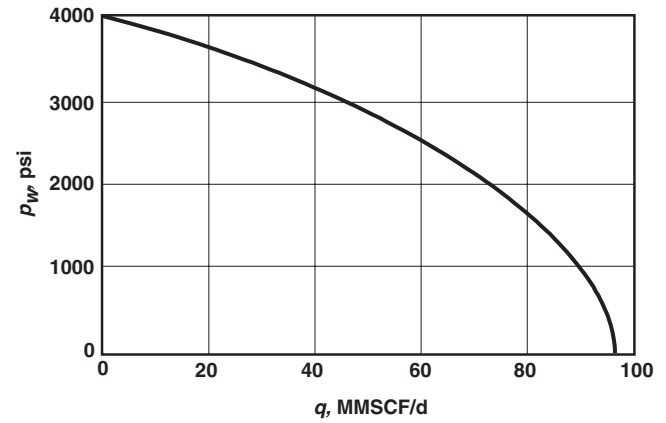


**Figure 19-10** Inflow performance of the fractured gas reservoir, non-Darcy effect from the Firoozabadi - Katz correlation

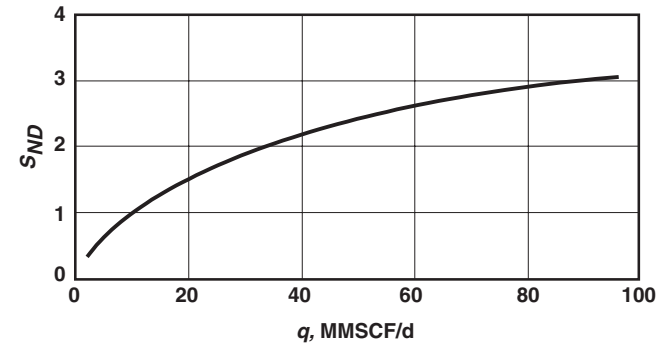


**Figure 19-11** Additional skin effect from non-Darcy flow in the fracture

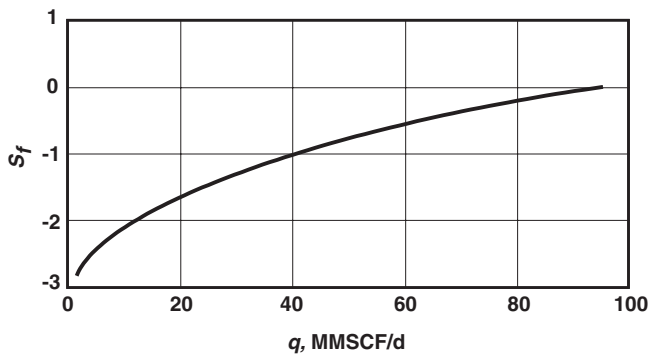


**Figure 19-12** Observable pseudoskin, the resulting effect of the fracture with non-Darcy flow effect

tive observable skin effect, while directly attributable to the inevitable effect of non-Darcy flow, might be interpreted as an unsuccessful HPF job.

## 19-7 SLOPES ANALYSIS

Complete tip-screenout is expected to produce a distinct behavior in the treating pressure; that is, the treating pressure should markedly increase with time. However, HPF treatments often exhibit numerous increasing-pressure intervals that are interrupted by anomalous pressure decreases, most probably because fracture extension can still occasionally occur (in many cases, a single complete tip-screenout is not achieved).

This work (Valkó *et al.*, 1996) provides a simple tool for examining such behavior. Treating-pressure curves are analyzed to gain insight to the evolution of fracture extent and a plausible end-of-job proppant distribution.

In developing the tool, several design parameters were intentionally imposed: the method should require minimum user input beyond the real treatment data, it should be relatively independent of the fracture propagation model used, and it should not be a history-matching procedure. In accordance with the basic requirement of model independence, the slopes analysis method is a screening tool based on simple equations and a well-defined (reconstructible) algorithm. Based on its simplicity, the tool lends itself to real-time use as well.

### 19-7.1 Assumptions

During tip-screenout, the fracture width is inflated while the area of the fracture faces remains theoretically constant. This phenomenon should appear as a marked increase in the treating pressure. In practice, the increasing pressure intervals may be interrupted by an anomalous pressure decrease because fracture extension can still occur occasionally. Based on this rationale, the HPF treatment is considered a series of (regular) arrested extension/width growth intervals interrupted by (irregular) fracture-area extension intervals.

In this case, the treatment can be decomposed into sequential periods of constant fracture area separated by periods (possibly several) of fracture extension. The time periods are located by a simple processing of the treatment-pressure curve.

If this vision of the treatment is accepted, then the slope of the increasing-pressure curve during a width-inflation period may be interpreted to obtain the “pack-

ing radius” of the fracture at that point during the treatment, which is characteristic for the given period. Putting together a sequence of packing-radii estimates gives a scenario which—combined with additional information on the proppant injection history—yields the final proppant distribution.

In transforming the idea to a working algorithm, several assumptions must be made, both regarding fracture geometry and the character of the leakoff process. The following assumptions are made:

- The created fracture is vertical with a radial geometry.
- Fluid leakoff can be described by the Carter leakoff model (Howard and Fast, 1957) in conjunction with the power-law type area growth used by Nolte (1979), or by one of the detailed leakoff models discussed in Section 19-3.3.
- Fracture-packing radius may increase or decrease with time.
- Hydraulic-fracture radius (which defines leakoff area) cannot decrease; it is the maximum of the packing radii that have occurred up to the given time.
- During regular width-inflation periods, the pressure slope is defined by linear, elastic rock behavior and fluid-material balance with friction effects being negligible.
- Injected proppant is distributed evenly along the actual packing area during each incremental period of arrested extension/width growth.

The suggested method consists of several steps. First, those portions of the bottomhole pressure curve are selected that show positive slope. The slope is then interpreted assuming that the pressure increase is caused by width inflation. The interpretation results in a packing radius that corresponds to a given time point. A step-by-step processing of the entire curve gives a history of the packing radius, though it still does not provide information regarding those intervals when the slope is negative. The history is made complete by interpolating between the known values.

Based on this history of packing-radius evolution, the final proppant distribution is easily determined by superimposing real-time proppant injection data. Final proppant distribution (which implies fracture length and width) is the practical result of the proposed slopes analysis.

### 19-7.2 Restricted-Growth Theory

Tip-screenout can be considered to be inflating the fracture width while the area of the fracture face does not increase. If the average width is denoted by  $w$  and the fracture-face area (one wing, one face) is denoted by  $A$ , then

$$\frac{dw}{dt} = \frac{1}{A}(i - q_L) \quad (19-49)$$

where  $i$  is the injection rate (per one wing) and  $q_L$  is the fluid-loss rate (from one wing).

The basic notation is shown in Figure 19-13. Assuming that the fracture is radial with radius  $R$ , then

$$A = \frac{\pi R^2}{2} \quad (19-50)$$

As a first approximation, assume that the pressure in the inflating fracture does not depend on location (it is homogeneous). The net pressure (the excess pressure above the minimum principal stress) is directly proportional to the average width:

$$p_n = \frac{3\pi E'}{16R} w \quad (19-51)$$

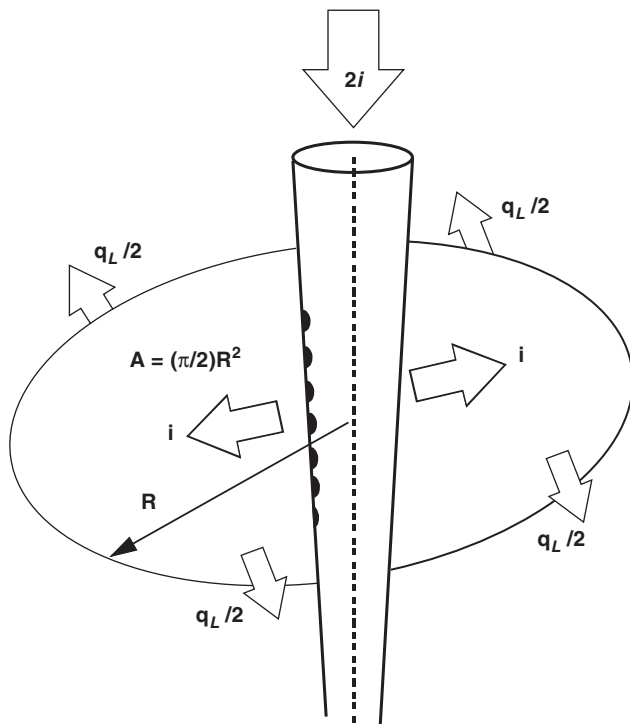


Figure 19-13 Schematic of fracpack, radial-fracture geometry

where  $E'$  is the plane-strain modulus (Chapter 17).

Substituting Equations 19-50 and 19-51 into Equation 19-49, the time derivative of net pressure is obtained as

$$\frac{dp}{dt} = \left(\frac{3\pi E'}{16R}\right)\left(\frac{2}{\pi R^2}\right)(i - q_L) \quad (19-52)$$

where the subscript for net pressure is dropped because the derivative of bottomhole pressure and that of net pressure are equal.

Recording the bottomhole pressure and injection rate provides the possibility of using Equation 19-52 to determine  $R$ . For this purpose, an estimate of  $q_L$  is needed.

Details of the Carter leakoff model are given in Chapter 17. Assuming that the fracture has extended up to the given time  $t$  according to Nolte's power-law assumption, and that it is arrested at the given time instant  $t$ , the leakoff rate  $q_{L,t}$  immediately after the arrest is given by

$$q_{L,t} = 2AC_L \frac{1}{\sqrt{t}} \left( \frac{\partial g(\Delta t_D, \alpha)}{\partial \Delta t_D} \right)_{\Delta t_D=0} \quad (19-53)$$

where  $A$  is the current fracture area and  $\alpha$  is the power-law exponent of the areal growth. The two-variable  $g$ -function was discussed in Chapter 17.

For a radial fracture created by injection of a Newtonian fluid, the exponent is taken as  $\alpha = \frac{8}{9}$ , and the derivative of the  $g$ -function is

$$\left[ \frac{\partial g(\Delta t_D, \frac{8}{9})}{\partial \Delta t_D} \right]_{\Delta t_D=0} = 1.91 \quad (19-54)$$

Therefore, the estimate of leakoff rate is obtained as

$$q_{L,t} = 2AC_L \frac{1}{\sqrt{t}} 1.91 \quad (19-55)$$

Equations 19-52 and 19-55 were developed explicitly in the text, and they form the core basis for the slopes analysis method. The use of these relations is demonstrated in the following section.

### 19-7.3 Slopes Analysis Algorithms

The restricted-growth theory is combined with simple material-balance computations to form the slopes analysis method as demonstrated below using a sample set of HPF data provided by Shell E&P Technology Co.

### 19-7.3.1 Selecting Intervals of Width Inflation

Figure 19-14 is the bottomhole pressure recorded during a HPF treatment. While it may look “not typical,” most of the data sets available (without the natural self-censoring of publishing authors) are “not typical” in one or more respects. The recommended approach of avoiding premature assumptions about the form of the pressure curve is based exactly on this fact. The slopes analysis approach can be better described as a signal processing operation than one of fitting a given model to the data.

The suggested method consists of selecting those portions of the bottomhole pressure curve that show positive slope. Straight lines are fitted to the points corresponding to each such interval.

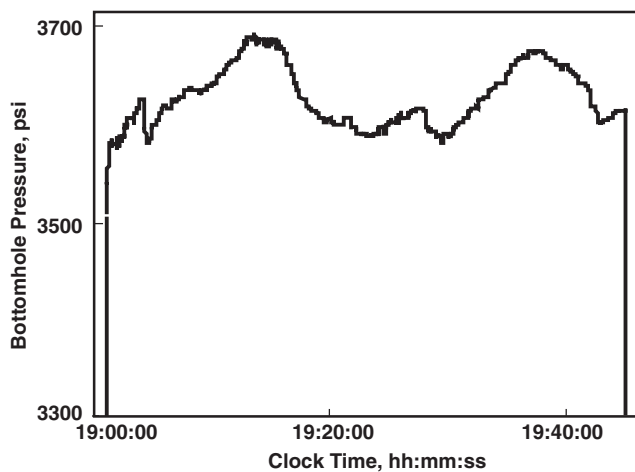


Figure 19-14 Bottomhole treating pressure from fracpack treatment

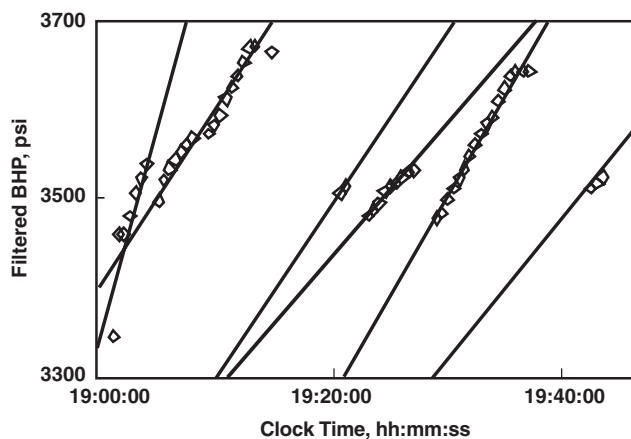


Figure 19-15 Bottomhole pressure points corresponding to width inflation intervals and corresponding “straight lines”

Using a simple algorithm, one can select points satisfying the criterion of restricted fracture growth. Straight lines are fitted to the individual series to arrive at the plot shown in Figure 19-15.

The slope of the straight line gives an average pressure derivative corresponding to the given time interval of restricted growth. In view of the stated assumptions, these slopes contain information that defines the actual packing radius corresponding to discrete moments during the HPF treatment.

### 19-7.3.2 Determining the Packing Radius Corresponding to a Width-Inflation Period

Substituting the obtained expression for the leakoff rate, Equation 19-52 can be rewritten as

$$m = \left( \frac{3\pi E'}{16R} \right) \left( \frac{2}{\pi R^2} \right) \left[ i - 2 \left( \frac{\pi R^2}{2} \right) C_L \frac{1}{\sqrt{t}} 1.91 \right] \quad (19-56)$$

Rearranging Equation 19-56, we obtain

$$R^3 + R^2 \left( \frac{2.25E' C_L}{m\sqrt{t}} \right) - \left( \frac{0.375E' i}{m} \right) = 0 \quad (19-57)$$

Once a restricted-growth interval is selected, knowing the slope,  $m$ , and the injection rate,  $i$  at a given time,  $t$ , Equation 19-57 can be solved for  $R$ . Since the equation is cubic, an explicit solution can be given, which (in consistent units) is given by

$$R_p = \frac{0.7501}{m\sqrt{t}} \left[ a - C_L \times E' + \frac{(C_L \times E')^2}{a} \right] \quad (19-58)$$

where

$$a = \left[ 0.4443 \times E' i \times m^2 \times t^{3/2} - (C_L \times E')^3 \right]^{1/3} \quad (19-59)$$

Equations 19-58 and 19-59 can be used with the actual one-wing slurry injection rate,  $i$ , recorded at time  $t$ . The obtained solution is the *packing radius*. Figure 19-16 shows the packing radius obtained from recorded data of the example HPF treatment. As seen from the figure, after a certain pumping time (approximately 25 min), the packing radius begins to decrease. In other words, near the end of the treatment, only the near-wellbore part of the fracture was “packed.” This condition is consistent with the treatment objectives, and it was achieved by

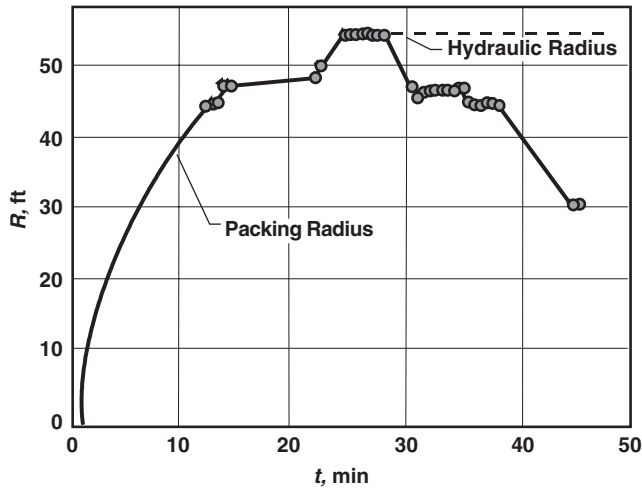


**Figure 19-16** Estimated packing radius with interpolation to fill in the “gaps”

gradually decreasing the injection rate at the final stages of the treatment.

### 19-7.3.3 Interpolation Between Known Values of the Packing Radius

Since the packing radius is obtained only in those selected intervals where width inflation can be assumed, a simple tool is needed to fill in the “gaps.” A simple logarithmic interpolation is used to estimate the packing radius in between the known values.

In addition, one can estimate the “hydraulic” fracture radius at time  $t$  as the maximum of the packing radii up to that point (dashed line in Figure 19-16). While proppant is placed within the actual packing radius, leakoff occurs along the area determined by the hydraulic-fracture extent. Knowledge of the hydraulic-fracture extent is useful for further material balance considerations.

### 19-7.3.4 Determining the Final Areal Proppant Concentration

Final proppant concentration (proppant distribution) in the fracture can be derived in a relatively straightforward fashion from the packing radius curve and knowledge of the bottomhole proppant concentration as a function of time. (The standard job record typically includes this information.)

Calculation of the final areal proppant concentration in the fracture follows the simple scheme:

1. For every time interval,  $\Delta t$ , determine the mass of proppant entering the fracture.
2. Assume this mass to be uniformly distributed inside the packing radius corresponding to the given time step.
3. Obtain the mass of proppant in a “ring” between radius  $R_1$  and  $R_2$  by summing up (accumulating) the mass of proppant placed during the whole treatment.
4. Repeat Step 3 for all rings to obtain the areal proppant concentration as a function of radial location  $R$ .

Application of the scheme above to the example data results in the areal proppant concentration as a function of the radial distance from the center of the perforations,  $R$ . The areal proppant concentration distribution for the example dataset is shown in Figure 19-17.

The proposed method for evaluating pressure behavior of HPF treatments is not based on specific fracture mechanics and/or proppant transport models. Rather, it takes the pressure curve “as is” and processes it using minimum additional data. The usual data records of a job (slurry injection rate, bottomhole proppant concentration, and bottomhole pressure) can be used for estimating fracture extent and the distribution of proppant in the fracture. The only other additional input parameters necessary for the analysis are plane-strain modulus and leakoff coefficient.

Success of the procedure depends on the validity of the key assumption that positive slopes observed in the bottomhole pressure curve are caused by restricted fracture extension/width growth. If there is no time interval satisfying the criterion of restricted extension or if no other phenomena involved mask the effect, such as (1) pressure

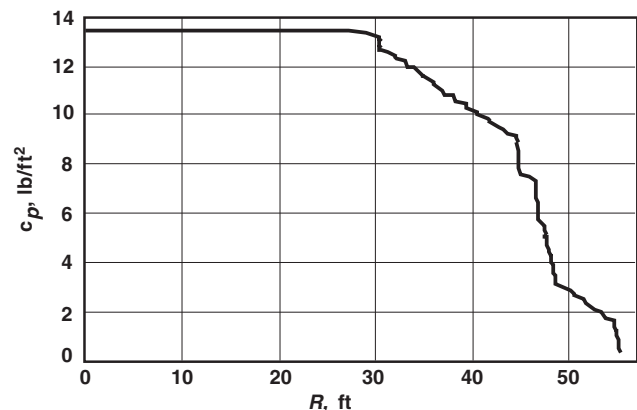


**Figure 19-17** Final areal proppant concentration as a function of radial distance from the center of the perforations

transients caused by sharp changes of the injection rate or (2) dramatic changes in friction pressure resulting from proppant concentration changes, the estimated packing radius might be in considerable error. Nevertheless, the suggested procedure is considered a substantive first step in the analysis of HPF treatment pressure data.

## 19-8 EMERGING HPF TECHNOLOGIES

### 19-8.1 Screenless and Rigless HPF Completions

On the basis of a recent industry survey, Tiner *et al.* (1996) report that the most common HPF technology advance being sought by producing companies is one that will allow removal or simplification of gravel-pack screens and tools, which are still used in most HPF completions. The most likely alternative is to eliminate the screen completely and use conventional fracturing methods, with a “twist”: the final proppant stage should be tailed-in with resin-coated sand to control proppant flowback. A number of these screenless HPF treatments have been completed, apparently with considerable success (Kirby *et al.*, 1995).

Screenless HPFs have the potential of dramatically reducing treatment costs and simplifying treatment execution; however, some questions remain: Can the resin-coated proppant in fact be placed as needed to prevent proppant flowback and ensure a high-conductivity connection between the fracture and the wellbore? What about formation sand production from those perforations that are not connected to the fracture? If successful, screenless HPFs would also allow the development of multiple-zone HPF completions and through-tubing HPF recompletions. The major benefit of through-tubing completions, of course, is that they can often be done without a rig on location.

New HPF operations and equipment are also emerging to allow rigless coiled tubing completions in wells that are completed with gravel-pack screens (Ebinger, 1996). Depending on the particular configuration, the treatment is pumped through a fracturing port/sleeve located below the production packer and above the screen. The port is opened and closed with a shifting tool on the coiled tubing. Because a gravel pack cannot be circulated into place, prepacked screens are required. This requirement seems to be the largest drawback to the technique. While the rigless HPFs may be uniquely suited to dual-zone completions, the primary influence behind this trend is cost reduction by eliminating rig costs and inefficiencies associated with rig timing.

### 19-8.2 Complex Well-Fracture Configurations

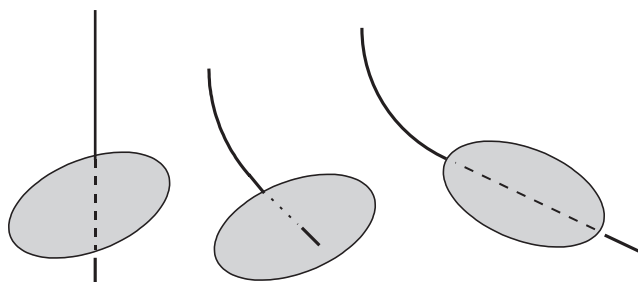
Vertical wells are not the only candidates for hydraulic fracturing. Figure 19-18 shows some basic configurations for single-fractured wells. Horizontal wells using HPF with the well drilled in the expected fracture azimuth (thereby ensuring a longitudinal fracture) appear to be (at least conceptually) a very promising prospect as discussed in Section 19-2.3. However, a horizontal well intended for a longitudinal fracture configuration would have to be drilled along the maximum horizontal stress. This requirement, in addition to well-understood drilling problems, may contribute to long-term stability problems.

Figure 19-19 illustrates two multiple-fracture configurations. A rather sophisticated conceptual configuration would involve the combination of HPF with multiple-fractured vertical branches emanating from a horizontal parent well drilled above the producing formation. Of course, horizontal wells, being normal to the vertical stress, are generally more prone to wellbore stability problems. Such a configuration would allow for placement of the horizontal borehole in a competent, nonproducing interval. Besides, there are advantages to fracture-treating a vertical section over a highly deviated or horizontal section: (1) multiple starter fractures, fracture turning, and tortuosity problems are avoided, (2) convergence-flow skins (“choke” effects) are much less of a concern, and (3) the perforating strategy is simplified.

### 19-8.3 Technology Demands: Where Do We Go From Here?

#### 19-8.3.1 Candidate Selection

Wellbore stability is viewed in a holistic approach with horizontal wells and hydraulic fracture treatments. Proactive well completion strategies are critical in well-



**Figure 19-18** Single-fracture configurations for vertical and horizontal wells

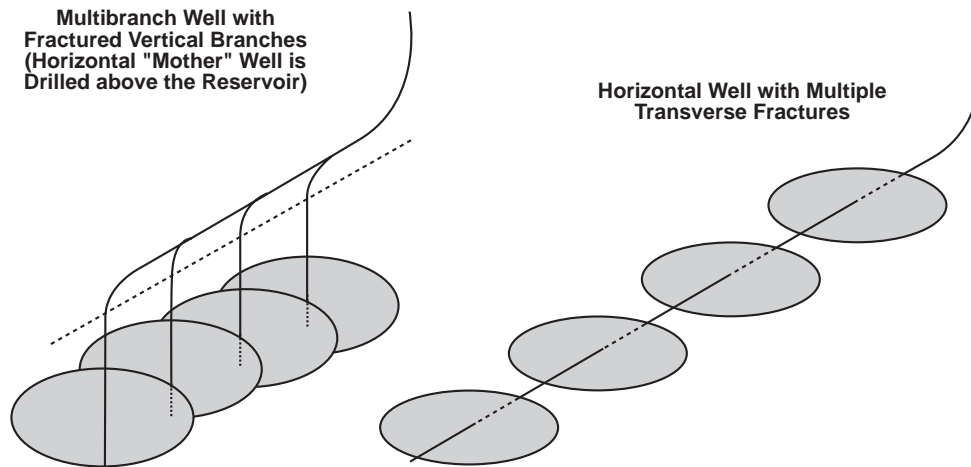


**Figure 19-19** Multibranch, multiple-fracture configurations for horizontal wells

bore stability and sand-production control to reduce drawdown while obtaining economically attractive rates. Reservoir candidate recognition for the correct well configurations is the critical element. Necessary steps in candidate selection include (1) appropriate reservoir engineering, (2) formation characterization using modern techniques, (3) wellbore-stability calculations, and (4) the substantive combination of production forecast with an assessment of sand-production potential. The mixed origin of the HPF (fracpack) community (gravel-packing and fracturing) still exists. For gravel-packers, it is still difficult to consider correctly the whole reservoir and not merely the near-wellbore region. On the other hand, for practitioners of fracturing, it is still difficult to understand the mechanisms involved in sanding and its control.

### 19-8.3.2 Completion Hardware

Completion hardware should be improved. As discussed above, there is a need to simplify, eliminate, or otherwise advance beyond the modified gravel-pack hardware currently being used in HPF. There is also a need for improved zonal isolation hardware, (for the execution of hydraulic fracturing in complex well-fracture configurations). In fact, lack of appropriate drilling, completion, and stimulation hardware is often the limiting factor in the indicated new completion configurations. Clearly, all fracture treatments must be conducted separately, in stages. Thus, inexpensive and robust zonal isolation schemes are necessary. Certain zonal-isolation hardware is available, but it is expensive and often logis-

tically difficult to use. Other currently available techniques such as polymer or sand plugs, are prone to failure.

### 19-8.3.3 The Fracture-Well Connection

New fracture-and-well interfaces should be developed, which could include the next generation of screens and replacement technologies. Hydraulic fractures are prone to sand production, both from the reservoir and the proppant-pack itself. This situation is particularly important in high-rate wells where, although the reservoir problem may be resolved, the near-well fracture portion may be susceptible to sand production. The current solution (gravel-pack screens) should be abandoned. Although they are reasonably effective, these screens can cause a serious choke effect at the fracture-well interface. New consolidation techniques or perhaps, oriented long perforations and alternative “sieves” can be envisioned.

### 19-8.3.4 Next-Generation Completion Fluids

The next generation of drilling and well completion fluids should also be developed. The envisioned “smart” fluids would consider application and formation-specific issues affecting wellbore stability and damage. New gels, polymers, and leakoff-control additives are urgently needed for the drilling of complicated wellpaths through difficult formations. Nondamaging fluids will be critical to the future of production engineering. Stimulation is often expensive, cumbersome, and at times, unsuccessful. Production-induced problems such as paraffin and asphaltene deposition, and

especially sand production, can be avoided if the well is undamaged, and no large drawdown is necessary for appropriate production.

#### 19-8.3.5 Treatment-Pressure Analysis

Treatment-pressure analysis is based on understanding the leakoff process and on the concept of net pressure. Soft formations and their rock mechanics are still not well understood, and an understanding of which mechanisms control fracture length and width is more evasive than ever. Many of the debates could be settled by determining the closure pressure (and hence the net pressure) with more confidence. While there is a lot of activity in this area, new results are very limited. Reiterating old ideas is common—(flowback or not, two minifrac or three, crosslinked fluid or not, step-rate or not, where to draw the straight line, etc.)—but these ideas are revealing little new information. There is definitely a need for innovative thinking here. For example, an independent and possibly direct instrumental determination of closure pressure would be a significant step ahead in the engineering of hydraulic fracturing in general, and especially for the hydraulic fracturing of soft formations.

#### 19-8.3.6 Improved Well Test Interpretation for HPF

From the point of view of evaluating high-permeability fracture treatments, it is imperative to improve the well-test interpretation procedure and understand the phenomenon of positive apparent skins. The lack of desired (negative) post-treatment skins is still haunting the industry. Well productivity is obviously being improved by HPF, but it is not clear whether the treatments are optimum or whether they could be significantly improved through the use of more aggressive treatment parameters. Would more aggressive schedules provide additional benefit, or are the possibilities limited by choke effect at the perforations? These issues are not clearly distinguished by current pressure-transient methods.

#### 19-8.3.7 Global Databases

There is an emerging consensus as to the importance of global databases of formation and other properties, at least for a specific geographic area and specific activity. The main difficulty is not to find funding for such data-

bases, but to provide incentive and methods to encourage continuous input of data and the tailoring of data formats toward common standards. Once a database is established, simple evaluation tools (such as the slopes-analysis method presented) can be used to evaluate a large number of treatments efficiently. Estimated fracture dimensions and conductivities could then be compared with results from pressure-transient analysis and production results. Discrepancies should be resolved using a large number of data sets from various independent sources.

## REFERENCES

- Aggour T.M., and Economides, M.J.: "Impact of Fluid Selection on High-Permeability Fracturing," paper SPE 36902, 1996.
- Ayoub, J.A., Kirksey, J.M., Malone, B.P., and Norman, W.D.: "Hydraulic Fracturing of Soft Formations in the Gulf Coast," paper SPE 23805, 1992.
- Balen, R.M., Meng, H.-Z. and Economides, M.J.: "Application of the Net Present Value (NPV) in the Optimization of Hydraulic Fractures," paper SPE 18541, 1988.
- Barree, R.D., Rogers, B.A., and Chu, W.C.: "Use of Frac-Pac Pressure Data to Determine Breakdown conditions and Reservoir Properties," paper SPE 36423, 1996.
- Brown, J.E., King, L.R., Nelson, E.B., and Ali, S.A.: "Use of a Viscoelastic Carrier Fluid in Frac-Pack Applications," paper SPE 31114, 1996.
- Chapman, B.J., Vitthal, S., and Hill, L.M.: "Prefacturing Pump-In Testing for High-Permeability Formations," paper SPE 31150, 1996.
- Chudnovsky, A., Fan J., Shulkin, Y., Dudley, J.W., Shlyapobersky, J, and Schraufnagel, R.: "A New Hydraulic Fracture Tip Mechanism in a Statistically Homogeneous Medium," paper SPE 36442, 1996.
- Cinco-Ley, H., and Samaniego, V.F.: "Transient Pressure Analysis: Finite Conductivity Fracture Case Versus Damage Fracture Case," paper SPE 10179, 1981.
- Cinco-Ley, H., Samaniego, V.F., and Dominquez, N.: "Transient Pressure Behavior for a Well With a Finite Conductivity Vertical Fracture," *SPEJ* (Aug. 1978) 253–264.
- Cinco-Ley, H., and Samaniego, V.F.: "Transient Pressure Analysis for Fractured Wells," *JPT* (Sept. 1981) 1749-1766.
- DeBonis, V.M., Rudolph, D.A., and Kennedy, R.D.: "Experiences Gained in the Use of Frac-Packs in Ultra-Low BHP Wells, U.S. Gulf of Mexico," paper SPE 27379, 1994.
- Dusterhoft, R., Vitthal, S., McMechan, D., and Walters, H.: "Improved Minifrac Analysis Technique in High-Permeability Formations," paper SPE 30103, 1995.
- Ebinger, C.D.: "New Frac-Pack Procedures Reduce Completion Costs," *World Oil* (April 1996).

- Ely, J.W.: *Stimulation Engineering Handbook*, Pennwell, Houston (1994).
- Fan, Y., and Economides, M.J.: "Fracturing Fluid Leakoff and Net Pressure Behavior in Frac&Pack Stimulation," paper SPE 29988, 1995.
- Firoozabadi, A., and Katz, D.L.: "An Analysis of High-Velocity Gas Flow Through Porous Media," *JPT* (Feb. 1979) 211-216.
- Gringarten, A.C., and Ramey, A.J., Jr.: "Unsteady State Pressure Distributions Created by a Well With a Single-Infinite Conductivity Vertical Fracture," *SPEJ* (Aug. 1974) 347-360.
- Grubert, D.M.: "Evolution of a Hybrid Frac-Gravel Pack Completion: Monopod Platform, Trading Bay Field, Cook Inlet, Alaska," paper SPE 19401, 1990.
- Guppy, K.H., Cinco-Ley, H., Ramey Jr., H.J., and Samaniego-V., F.: "Non-Darcy Flow in Wells With Finite-Conductivity Vertical Fractures," *SPEJ* (Apr. 1982) 681-698; **Trans., AIME** 273.
- Hannah, R.R., Park, E.I., Walsh, R.E., Porter, D.A., Black, J.W., and Waters, F.: "A Field Study of a Combination Fracturing/Gravel Packing Completion Technique on the Amberjack, Mississippi Canyon 109 Field," paper SPE 26562, 1993.
- Howard G.C., and Fast, C.R.: "Optimum Fluid Characteristics for Fracture Extension," *Drill. and Prod. Prac.*, API (1957) 261-270.
- Hunt, J.L., Chen, C.-C., and Soliman, M.Y.: "Performance of Hydraulic Fractures in High-Permeability Formations," paper SPE 28530, 1994.
- Kirby, R.L., Clement, C.C., Asbill, S.W., Shirley, R.M., and Ely, J.W.: "Screenless Frac Pack Completions Utilizing Resin Coated Sand in the Gulf of Mexico," paper SPE 30467, 1995.
- Lacy, L.L., Rickards, A., and Bilden, D.M.: "Fracture Width and Embedment Testing in Soft Reservoir Sandstone," paper SPE 36421, 1996.
- Martins, J.P., Collins, P.J., and Rylance, M.: "Small Highly Conductive Fractures Near Reservoir Fluid Contacts: Application to Prudhoe Bay" paper SPE 24856, 1992.
- Mathur, A.K., Ning, X., Marcinew, R.B., Ehlig-Economides, C.A., and Economides, M.J.: "Hydraulic Fracture Stimulation of High-Permeability Formations: The Effect of Critical Fracture Parameters on Oilwell Production and Pressure," paper SPE 30652, 1995.
- Mayerhofer, M.J., Economides, M.J., and Nolte, K.G.: "An Experimental and Fundamental Interpretation of Fracturing Filter-Cake Fluid Loss," paper SPE 22873, 1991.
- Mayerhofer, M.J., Economides, M.J., and Ehlig-Economides, C.A.: "Pressure Transient Analysis of Fracture Calibration Tests," paper SPE 26527, 1993.
- McLarty, J.M., and DeBonis, V.: "Gulf Coast Section SPE Production Operations Study Group - Technical Highlights from a Series of Frac Pack Treatment," paper SPE 30471, 1995.
- McGuire W.J., and Sikora, V.J.: "The Effect of Vertical Fractures on Well Productivity," *JPT* (Oct. 1960) 72.
- McGowen, J.M., Vitthal, S., Parker, M.A., Rahimi, A., and Martch Jr., W.E.: "Fluid Selection for Fracturing High-Permeability Formations," paper SPE 26559, 1993.
- McGowen J.M., and Vitthal S.: "Fracturing Fluid Leakoff Under Dynamic Conditions Part 1: Development of a Realistic Laboratory Testing Procedure," paper SPE 36492, 1996.
- Montagna, J.N., Saucier, R.J., and Kelly, P.: "An Innovative Technique for Damage By-Pass in Gravel Packed Completions Using Tip Screenout Fracture Prepacks," paper SPE 30102, 1995.
- Monus, F.L., Broussard, F.W., Ayoub, J.A., and Norman, W.D.: "Fracturing Unconsolidated Sand Formations Offshore Gulf Mexico," paper SPE 22844, 1992.
- Mullen, M.E., Norman, W.D., and Granger, J.C.: "Productivity Comparison of Sand Control Techniques Used for Completions in the Vermilion 331 Field," paper SPE 27361, 1994.
- Mullen, M.E., Norman, W.D., Wine, J.D., and Stewart, B.R.: "Investigation of Height Growth in Frac Pack Completions," paper SPE 36458, 1996.
- Mullen, M.E., Stewart, B.R., and Norman, W.D.: "Evaluation of Bottomhole Pressures in 40 Soft Rock Frac-Pack Completions in the Gulf of Mexico," paper SPE 28532, 1994.
- Nolte, K.G.: "Determination of Proppant and Fluid Schedules from Fracturing Pressure Decline," *SPEPE* (July 1986) 255-265; also paper SPE 8341, 1979.
- Ning, X., Marcinew, R.P., and Olsen, T.N.: "The Impact of Fracturing Fluid Cleanup and Fracture-Face Damage on Gas Production," paper CIM 95-43, 1995.
- Patel, Y.K., Troncoso, J.C., Saucier, R.J., and Credeur, D.J.: "High-Rate Pre-Packing Using Non-Viscous Carrier Fluid Results in Higher Production Rates in South Pass Block 61 Field," paper SPE 28531, 1994.
- Reimers, D.R., and Clausen, R.A.: "High-Permeability Fracturing at Prudhoe Bay, Alaska," paper SPE 22835, 1991.
- Roodhart, L.P.: "Fracturing Fluids: Fluid-Loss Measurements Under Dynamic Conditions," *SPEJ* (Oct. 1985) 629-636.
- Roodhart, L.P., Fokker, P.A., Davies, D.R., Shlyapobersky, J., and Wong, G.K.: "Frac and Pack Stimulation: Application, Design, and Field Experience From the Gulf of Mexico to Borneo," paper SPE 26564, 1993.
- Saucier, R.J.: "Considerations in Gravel Pack Design," *JPT* (Feb. 1974) 205212.
- Singh, P.K., and Agarwal, R.G.: "Two-Step Rate Test: A New Procedure for Determining Formation Parting Pressure," paper SPE 18141, 1988.
- Smith, M.B., Miller II, W.K., and Haga, J.: "Tip Screenout Fracturing: A Technique for Soft, Unstable Formation," *SPEPE* (May 1987) 95-103.
- Stewart, B.R., Mullen, M.E., Ellis, R.C., Norman, W.D., and Miller, W.K.: "Economic Justification for Fracturing Moderate to High-Permeability Formations in Sand Control Environments," paper SPE 30470, 1995a.

- Stewart, B.R., Mullen, M.E., Howard, W.J., and Norman, W.D.: "Use of a Solids-free Viscous Carrying Fluid in Fracturing Applications: An Economic and Productivity Comparison in Shallow Completions," paper SPE 30114, 1995b.
- Tiner, R.L., Ely, J.W., and Schraufnagel, R.: "Frac Packs — State of the Art," paper SPE 36456, 1996.
- Valkó, P., Oligney, R.E., and Schraufnagel, R.A.: "Slopes Analysis of Frac & Pack Bottomhole Treating Pressures," paper SPE 31116, 1996.
- Valkó, P., and Economides, M.J.: "Performance of Fractured Horizontal Wells in High-Permeability Reservoirs," paper SPE 31149, 1996.
- van Poolen, H.K., Tinsley, J.M., and Saunders, C.D.: "Hydraulic Fracturing—Fracture Flow Capacity vs. Well Productivity" *Trans. AIME* (1958) **213**, 91.
- Vitthal S., and McGowen J.M.: "Fracturing Fluid Leakoff Under Dynamic Conditions Part 2: Effect of Shear Rate, Permeability and Pressure," paper SPE 36493, 1996.
- Wattenburger, R.A., and Ramey Jr., H.J.: "Well-Test Interpretation of Vertically Fractured Gas Wells," paper SPE 2115, 1969.
- Wong, G.K., Fors, R.R., Casassa, J.S., Hite, R.H., Wong, G.K., and Shlyapobersky, J.: "Design, Execution and Evaluation of Frac and Pack (F&P) Treatments in Unconsolidated Sand Formations in the Gulf of Mexico," paper SPE 26564, 1993.